Numerical Solutions of Wave Propagation in Beams

by

Ryan William Tschetter

A Thesis Presented in Partial Fulfillment
of the Requirements for the Degree
Master of Science

Approved April 2016
Graduate Supervisory Committee:

Keith Hjelmstad, Chair
Subramaniam Rajan
Barzin Mobasher

ARIZONA STATE UNIVERSITY

May 2016

ABSTRACT

In order to verify the dispersive nature of transverse displacement in a beam, a deep understanding of the governing partial differential equation is developed. Using the finite element method and Newmark's method, along with Fourier transforms and other methods, the aim is to obtain consistent results across each numerical technique. An analytical solution is also analyzed for the Euler-Bernoulli beam in order to gain confidence in the numerical techniques when used for more advance beam theories that do not have a known analytical solution. Three different beam theories are analyzed in this report: The Euler-Bernoulli beam theory, Rayleigh beam theory and Timoshenko beam theory. A comparison of the results show the difference between each theory and the advantages of using a more advanced beam theory for higher frequency vibrations.

ACKNOWLEDGMENTS

The author would like to generously acknowledge the guidance of his graduate committee and all others who aided in the work competed herein. A special dedication goes out to Dr. Keith D. Hjelmstad for his generous consultations during the course of this study as well as recommending the problem of understanding and verifying the dispersion phenomenon that was discovered through numerical approximations to the beam equation. The author would also like to recognize Dr. Huei-Ping Huang for his assistance in understanding how to solve more complex partial differential equations and guidance in finishing the work of solving the fourth order, partial differential equation, analytically.

TABLE OF CONTENTS

Page

CHAPTER Page

LIST OF FIGURES

Figure Page

Figure Page

1 INTRODUCTION

As an engineering student, a professional engineer or an engineering professor, one question will always come up in the field of engineering, “Is the solution correct?” One important quality engineering student learn from undergraduate and graduate school is having an idea of what the solution should look like. When the solution does not match up with what was initially predicted, questions arise. The contents of this report are focused primarily on that exact problem.

In the “*Structural Dynamics*” course at Arizona State University, axial and transverse displacement in beams were analyzed using numerical methods. The axial bar problem had a simple analytical solution, and thus was simple to prove that the numerical solution was accurate. Using MATLAB, the axial bar problem was solved by implementing the finite element method and Newmark’s method. The solution showed a strong dependence on the numerical parameters (see Figure 1); the waves would disperse and behave in a manner that did not coincide with the analytical solution.

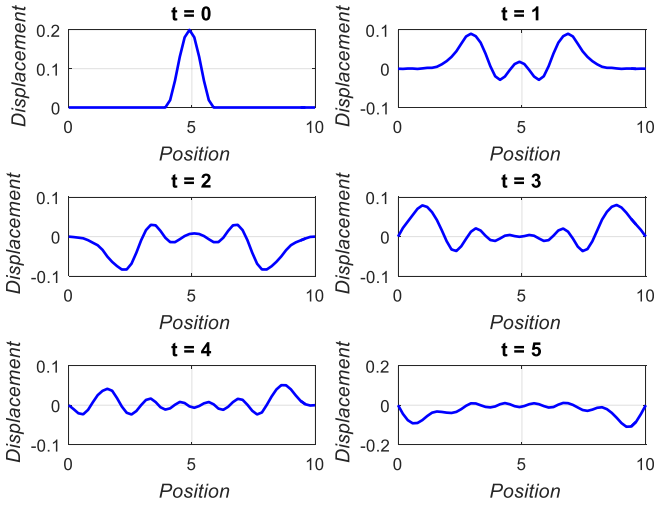

Figure 1: Axial Waves - 50 Elements - 0.01 Second Time Increment

The analytical solution to the axial bar suggests that the waves would propagate in a harmonic motion without dispersion. By adjusting the time step used in Newmark's method to more accurately approximate integrals, and by increasing the resolution of the spatial discretization, the numerical approach proved to match the analytical approach. Figure 2 shows the harmonic waves as expected when the level of spatial discretization is increased and the size of the time increment is decreased.

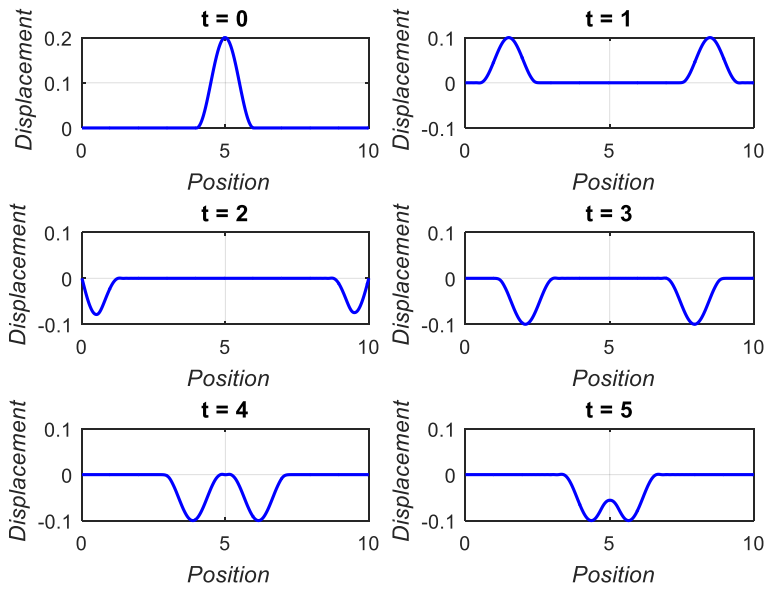

Figure 2: Axial Waves - 500 Elements - 0.001 Second Time Increment

After learning about wave propagation in the axial bar, attention was turned to transverse displacement in beams. There are multiple beam theories, but the main focus was aimed towards the Euler-Bernoulli beam theory and the Rayleigh beam theory which are derived and discussed in the following chapters. Using the same method incorporated to approximate the solution to the axial bar, the finite element method and Newmark's method were used to approximate the solution for transverse displacement in beams.

Figure 3 shows the initial displacement at multiple instances of time using a coarser, spatial discretization.

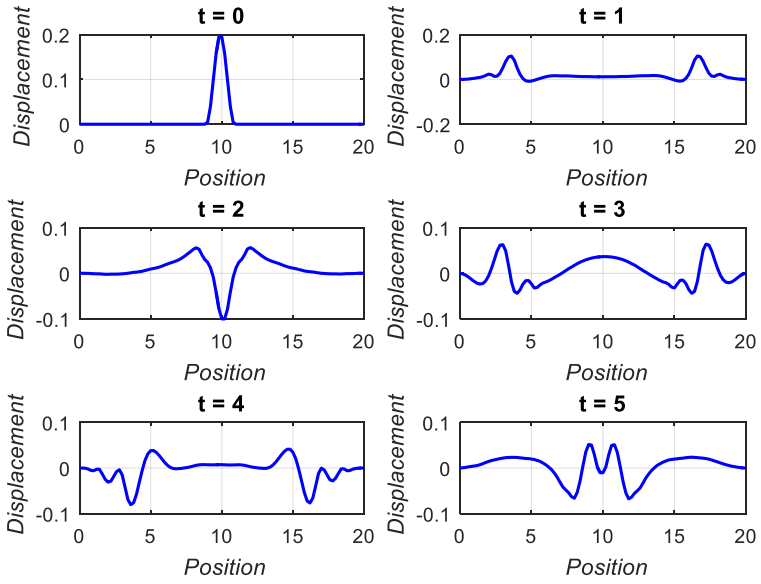

Figure 3: Transverse Waves - 100 Elements - 0.01 Second Time Increment

Increasing the level of spatial discretization and decreasing the size of the time step did have a fairly drastic effect on the shape of the wave. Figure 5 shows the graphical changes in the wave propagation due to the change in spatial discretization and time step.

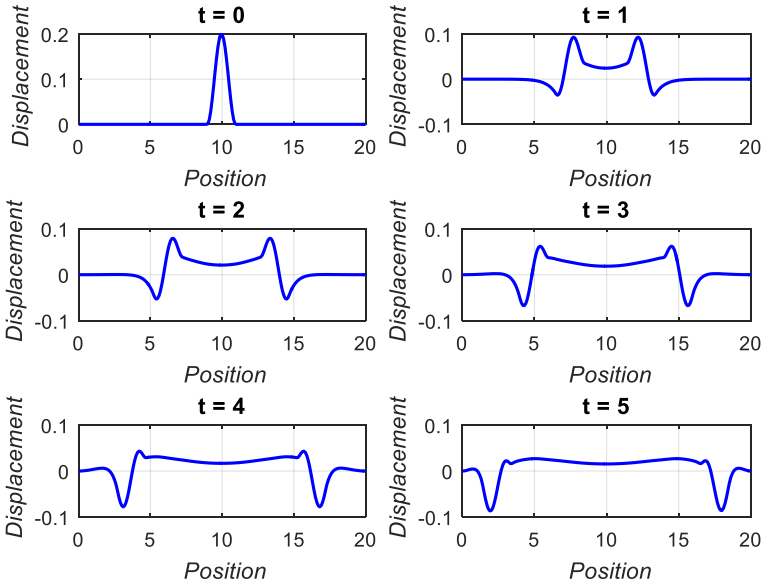

Figure 4: Transverse Waves - 200 Elements - 0.005 Second Time Increment

Although there was a drastic change shown between Figure 3 and Figure 5, further refinement of the time stepping method and spatial discretization proved to show little difference and appear to converge, as shown in Figure 5.

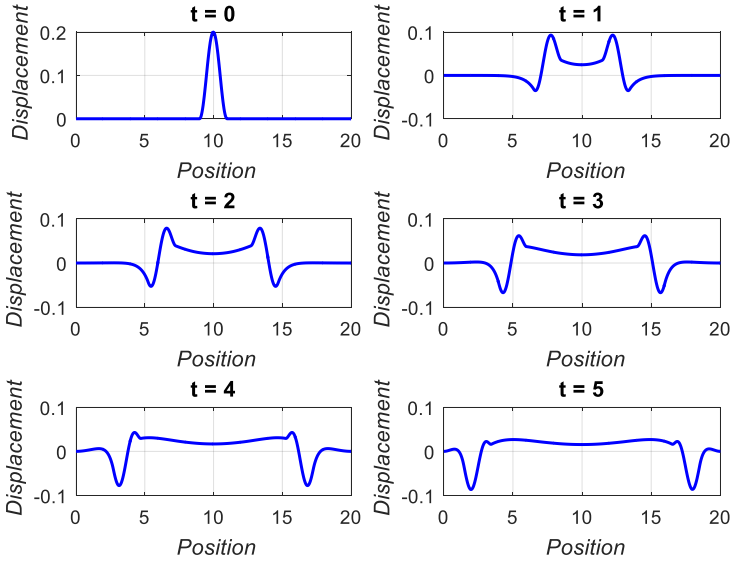

Figure 5: Transverse Waves - 500 Elements - 0.001 Second Time Increment

At first, the issue started out as a personal problem. Due to a lack of knowledge in partial differential equations, an analytical solution was not readily available to compare results to. After observing how the spatial discretization and the time step affected the results of the wave propagation for the axial bar problem, it was difficult to accept the dispersive shape shown in Figure 5 for transverse displacements.

It did not take long to find literature showing the dispersive nature that has been the rise of many questions. Figure 6 shows an interesting figure found in *Vibration and Sound* by Philip M. Morse. Using Fourier transforms and Laplace transforms, an analytical solution for the Euler-Bernoulli beam was obtained.

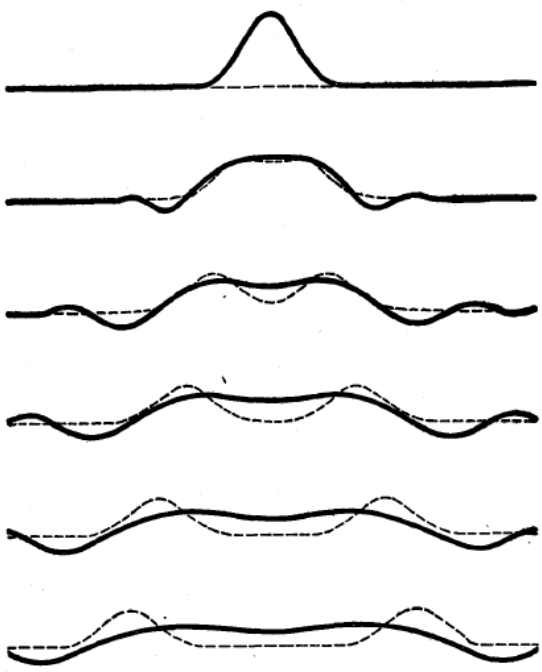

Figure 6: Dispersive Waves from the Analytical Solution to the Euler-Bernoulli Beam (Morse)

For successive instances of time, the transverse displacement of the Euler-Bernoulli beam is compared to the displacement shown by a "flexible string." The idea of the flexible string is similar to that of the axial bar as we can see the waves behave in the same manner. Seeing this result gave confidence that the finite element program created

in MATLAB was correct. Although this information was satisfying, more questions remained. The Fourier transform assumes the domain of the partial differential equation is infinite, where the beam in question had a finite domain. With an infinitely long beam, the effects of the boundary conditions cannot be analyzed. The other problem is that the solutions shown in Figure 6 was only for the Euler-Bernoulli beam, while verification for the Rayleigh beam is still desired.

More information about the dispersive waves was gathered by studying the dispersion relationship. The dispersion relationship is a well understood relationship to those who study partial differential equations and is discussed in much more detail in the coming chapters. The basic idea behind the dispersion relationship is that, for different wave propagation problems, the wave number and the wave speed are related in some fashion. If the wave speed is constant across different wave numbers, then no dispersion would occur. However, if the wave number is expressed as a non-constant function of the wave speed, then the waves would disperse.

After seeing other methods have comparable results to the finite element method, confidence was built that the finite element program was obtaining the correct solution. Along with an understanding of the dispersion relation, it was clearer that the beam waves would be dispersive. Although some questions have been answered through literature, more questions have come about. In order to truly verify that the finite element program is correct, the results must be repeatable using any method of numerical approximation. If different methods converge to the same solution for the same initial conditions, then a conclusion can be made that the solution is correct. However if the

results are not replicated using various solution techniques, this conclusion cannot be made; if the results are not repeatable, then it is not science.

2 BEAM THEORIES

In order to understand wave propagation, a clear understanding of the equation of motion is necessary. Depending on the assumptions being made, several different equations of motion can be derived. The three beam theories that will be studied throughout this report include: Euler-Bernoulli Beam Theory, Rayleigh Beam Theory and the Timoshenko Beam Theory. For all of these theories, several standard assumptions are noted:

A. The material is elastic, homogeneous and isotropic.
B. The beam is prismatic and symmetric about the principal axis.
C. Transverse deflections are small.

These assumptions allow for simplifications within the upcoming derivations such as being able to pull constant material and geometric properties out of integrals. These assumptions are standard across all three of the beam theories, however there are also a few assumptions that are unique to each individual beam theory.

2.1 The Euler-Bernoulli Beam Theory

The Euler-Bernoulli beam theory is the most elementary theory of those listed in this report. The following assumptions introduce important constraints that help simplify the problem at hand. The partial differential equations produced through the beam theories become more difficult to solve as the constraints are lifted. The constraints implemented to derive the Euler-Bernoulli beam equation are:

A. Rotational acceleration cause by rotational displacements are negligible.
B. Shear deformations are negligible.

The first assumption allows us to neglect the rotary inertia of the beam elements. Along with neglecting the shear deformation, the equation of motion is greatly simplified by these assumptions, yet still yields reasonable results for beam vibration.

Figure 7 shows the Euler-Bernoulli beam that will be used to create a generic equation of motion.

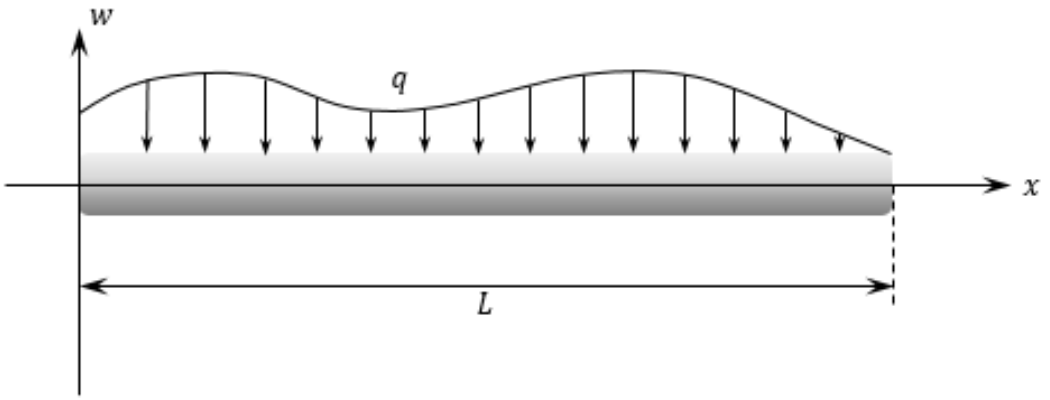

Figure 7: Euler-Bernoulli Beam

Figure 8 shows the individual element that will be examined. A representative element, shown in Figure 9 is used to create a loading diagram that is representative of the entire beam.

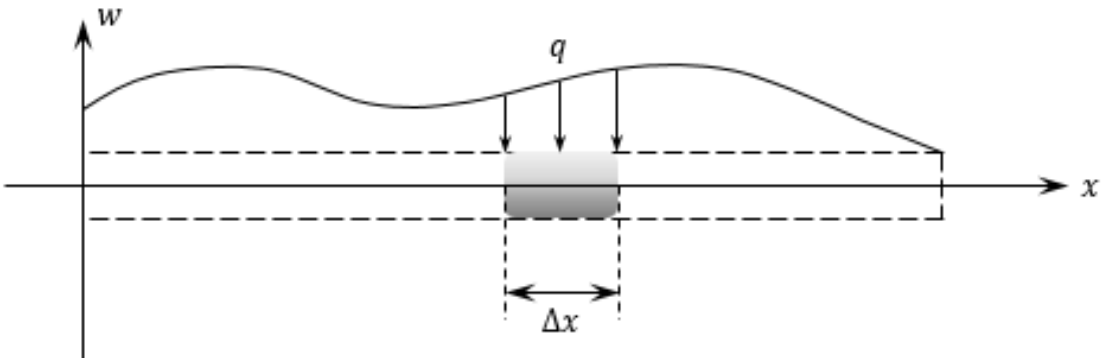

Figure 8: A Representative Element Within the Beam to be Examined

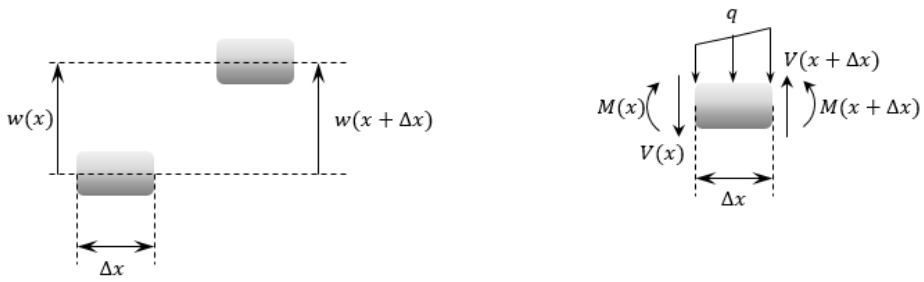

Figure 9: Loading Diagram of the Representative Element

Using Newton's second law of motion, the vertical forces are summed and set equal to the mass times the acceleration.

$$V(x+\Delta x) - V(x) - q \times \Delta x = \rho A \ddot{w} \Delta x \tag{1}$$

Here, ρ is the mass density per unit length and A is the cross sectional area of the beam. Dividing equation (1) by the length of the representative element, Δx

$$\frac{\partial V}{\partial x} - q = \rho A \ddot{w} \tag{2}$$

Due to the constraint the rotary inertia is negligible, the sum of the moments must equal zero.

$$M(x+\Delta x) - M(x) + V(x+\Delta x)\Delta x = 0 \tag{3}$$

Again, dividing equation (3) by the length of the representative element, Δx

$$V = -\frac{\partial M}{\partial x} \tag{4}$$

Taking the derivative of equation (4), then plugging into equation (2) results in

$$\frac{\partial^2 M}{\partial x^2} + \rho A \ddot{w} = -q \tag{5}$$

From the constraint that shear deformations are negligible and the plane section hypothesis, we know the moment is proportion to the second derivative of displacement.

$$\frac{\partial^2 w}{\partial x^2} = \frac{M}{EI} \rightarrow M = EI\frac{\partial^2 w}{\partial x^2} \rightarrow \frac{\partial^2 M}{\partial x^2} = EI\frac{\partial^4 w}{\partial x^4} \tag{6}$$

Combining equation (6) with equation (5) results in the Euler-Bernoulli beam equation

$$EI\frac{\partial^4 w}{\partial x^4} + \rho A\frac{\partial^2 w}{\partial t^2} = -q \tag{7}$$

Equation (7) will be used in the following chapters to model the Euler-Bernoulli beam and compare to the other two beam theories.

2.2 The Rayleigh Beam Theory

Unlike the Euler-Bernoulli beam theory, the rotary inertia will now be considered. Figure 10 shows the displacement and rotation of a representative beam element.

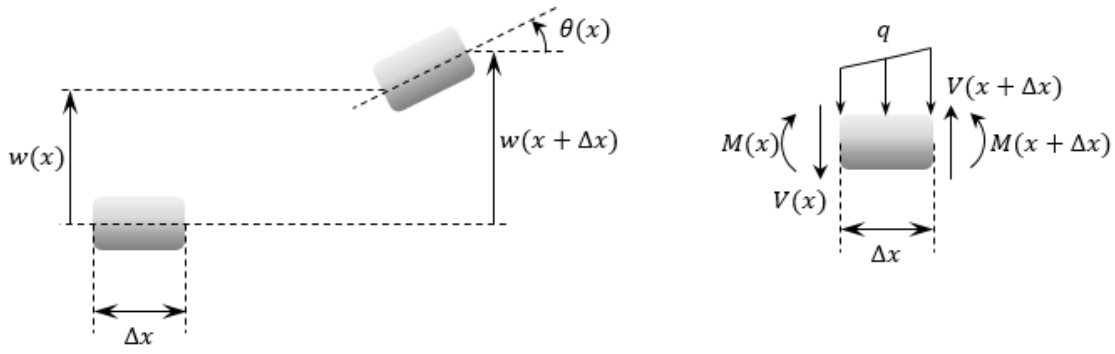

Figure 10: Displacement and Rotation of a Rayleigh Beam Element

Now that the element is rotating, the sum of the moments is no longer equal to zero. Instead, the sum of the moments must be proportional to the angular acceleration.

$$M(x + \Delta x) - M(x) + V(x + \Delta x)\Delta x = \rho I\ddot{\theta}dx \tag{8}$$

Here, I represents the moment of inertia and $\ddot{\theta}$ is the angular acceleration. Dividing equation (8) by the length of the representative element results in

$$V = \rho I\ddot{\theta} - \frac{\partial M}{\partial x} \tag{9}$$

Taking the derivative of equation (9), and substituting into equation (2) result in

$$\frac{\partial V}{\partial x} = \rho I\ddot{\theta}' - \frac{\partial^2 M}{\partial x^2} \rightarrow \frac{\partial^2 M}{\partial x^2} + \rho A\ddot{w} - \rho I\ddot{\theta}' = -q \tag{10}$$

From the constrain that shear deformations are negligible, it is known that for small displacements, $\theta = w' \rightarrow \ddot{\theta}' = \ddot{w}''$. Combining equation (6) and equation (10) yields the Rayleigh beam equation

$$EI\frac{\partial^4 w}{\partial x^4} - \rho I\frac{\partial^4 w}{\partial x^2 \partial t^2} + \rho A\frac{\partial^2 w}{\partial t^2} = -q \tag{11}$$

2.3 The Timoshenko Beam Theory

The Timoshenko beam theory will be the most complete beam theory discussed. Both of the assumptions in the Euler-Bernoulli beam theory are now taken care of as the Timoshenko beam theory takes into account both rotary motion and shear deformations. First, let's note that the shear force for the Timoshenko beam is represented as

$$V = G\theta A_s = GA_s\left(\frac{\partial w}{\partial x} - \psi\right) \tag{12}$$

Here, θ is the total rotation of the neutral fiber, equal to the sum of the rotation from transverse displacement, $\frac{\partial w}{\partial x}$ and the angle from the shear stress, ψ. A_s is a corrected area which includes a reduction factor to account for the non-uniform distribution of shear stress across the cross section of the beam. Let us also note that the moment can be represented as

$$M = EI\frac{\partial \psi}{\partial x} \tag{13}$$

Using Figure 10, the sum of the forces in the vertical direction must equal the mass of the element times the acceleration.

$$V(x+dx) - V(x) - qdx = \rho A \frac{\partial^2 w}{\partial t^2} dx \tag{14}$$

Dividing through by the length of the element results in

$$\frac{\partial V}{\partial x} - q = \rho A \frac{\partial^2 w}{\partial t^2} \tag{15}$$

Substituting equation (12) into (15) will yield

$$GA_s \left(\frac{\partial^2 w}{\partial x^2} - \frac{\partial \psi}{\partial x} \right) - \rho A \frac{\partial^2 w}{\partial t^2} = q \tag{16}$$

The next step will be to look at the rotational dynamics of the beam. Taking the sum of the moments about any point must equal the rotational inertia times the rotational acceleration.

$$\rho I \frac{\partial^2 \psi}{\partial t^2} dx = M(x+dx) - M + V(x+dx)dx \tag{17}$$

Dividing by the length of the representative element

$$\rho I \frac{\partial^2 \psi}{\partial t^2} = \frac{\partial M}{\partial x} + V \tag{18}$$

Substituting equations (12) and (13) into (18) gives the final equation of motion for the rotational dynamics.

$$\rho I \frac{\partial^2 \psi}{\partial t^2} = EI \frac{\partial^2 \psi}{\partial x^2} + GA_s \left(\frac{\partial w}{\partial x} - \psi \right) \tag{19}$$

Equations (16) and (19) make up the equation of motion for the entire system. Together, they are a coupled pair of partial differential equations. This system of equations can be taken a step further by eliminating ψ from the equations. For use in the finite element method, it is actually preferred to keep the system of partial differential

equations in order to derive the equation of motion. However, as we will see for the other methods, creating a single, higher order, partial differential equation actually aids in the solution process. Let's start by solving equation (16) for $\partial\psi/\partial x$. For free vibration, no external load is present, $q = 0$.

$$\frac{\partial\psi}{\partial x} = -\frac{\rho A}{GA_s}\frac{\partial^2 w}{\partial t^2} + \frac{\partial^2 w}{\partial x^2} \tag{20}$$

Then, let's differentiate equation (19) with respect to position.

$$\rho I\frac{\partial^3\psi}{\partial x\partial t^2} = EI\frac{\partial^3\psi}{\partial x^3} + GA_s\left(\frac{\partial^2 w}{\partial x^2} - \frac{\partial\psi}{\partial x}\right) \tag{21}$$

Now, substituting equation (20) into (21), we can eliminate the ψ term.

$$\begin{aligned}\rho I\left[-\frac{\rho A}{GA_s}\frac{\partial^4 w}{\partial t^4} + \frac{\partial^4 w}{\partial x^2\partial t^2}\right] \\ = EI\left[-\frac{\rho A}{GA_s}\frac{\partial^4 w}{\partial t^2\partial x^2} + \frac{\partial^4 w}{\partial x^4}\right] + GA_s\left(\frac{\partial^2 w}{\partial x^2} + \frac{\rho A}{GA_s}\frac{\partial^2 w}{\partial t^2} - \frac{\partial^2 w}{\partial x^2}\right)\end{aligned} \tag{22}$$

We can further distribute and group together like terms in order to simplify the equation.

$$\left(\rho I + \frac{\rho AEI}{GA_s}\right)\frac{\partial^4 w}{\partial x^2\partial t^2} - \frac{\rho^2 IA}{GA_s}\frac{\partial^4 w}{\partial t^4} = EI\frac{\partial^4 w}{\partial x^4} + \rho A\frac{\partial^2 w}{\partial t^2} \tag{23}$$

Dividing equation (23) by ρA will bring us to the final form of the Timoshenko beam equation.

$$\frac{\rho I}{GA_s}\frac{\partial^4 w}{\partial t^4} - \left(\frac{I}{A} + \frac{EI}{GA_s}\right)\frac{\partial^4 w}{\partial x^2\partial t^2} + \frac{EI}{\rho A}\frac{\partial^4 w}{\partial x^4} + \frac{\partial^2 w}{\partial t^2} = 0 \tag{24}$$

2.4 Beam Theory Summary

Now that the three important beam theories have been derived they can be used in the coming chapters to investigate the dispersion phenomenon. Here are the three equations that will be used:

- Euler-Bernoulli: Equation (7) - $EI\frac{\partial^4 w}{\partial x^4} + \rho A\frac{\partial^2 w}{\partial t^2} = 0$
- Rayleigh: Equation (11) - $EI\frac{\partial^4 w}{\partial x^4} - \rho I\frac{\partial^4 w}{\partial x^2 \partial t^2} + \rho A\frac{\partial^2 w}{\partial t^2} = 0$
- Timoshenko: Equation (24) - $\frac{\rho I}{GA_s}\frac{\partial^4 w}{\partial t^4} - \left(\frac{I}{A} + \frac{EI}{GA_s}\right)\frac{\partial^4 w}{\partial x^2 \partial t^2} + \frac{EI}{\rho A}\frac{\partial^4 w}{\partial x^4} + \frac{\partial^2 w}{\partial t^2} = 0$

To analyze free vibrations, the above equations have no external loading $q = 0$.

3 FOURIER ANALYSIS & AN ANALYTICAL SOLUTION

3.1 Euler-Bernoulli Beam Solution

The equation of motion given in equation (7) is a fourth order partial differential equation. This can be solved analytically through the use of Laplace transforms and Fourier transforms. Let's rewrite equation (7) in a more useful form.

$$k^2 \frac{\partial^4 w}{\partial x^4} + \frac{\partial^2 w}{\partial t^2} = 0 \tag{25}$$

Equation (25) combines the constants into a single term, $k = \sqrt{EI/\rho A}$ and considering the case of no externally applied load, $q = 0$. We will take note of the initial conditions that the position at time zero is equal to a generic function, $w(x, 0) = f(x)$. The velocity at time zero is equal to zero, $\dot{w}(x, 0) = 0$. Starting with taking the Laplace transform with respect to time, and letting $\mathcal{L}(w) = \overline{w} = \overline{w}(x, s)$, equation (25) becomes

$$k^2 \frac{\partial^4 \overline{w}}{\partial x^4} + s\big(s\overline{w} - w(0)\big) - \dot{w}(0) = 0 \rightarrow k^2 \frac{\partial^4 \overline{w}}{\partial x^4} + s^2 \overline{w} = sf(x) \tag{26}$$

The next step to solve the partial differential equation is by taking the Fourier transform with respect to x. For this, we will let $\mathcal{F}(\overline{w}) = \widetilde{\overline{w}} = \widetilde{\overline{w}}(\xi, s)$. Take note that we are invoking the derivative theorem, $\mathcal{F}(w') = -i\xi\mathcal{F}(w)$

$$k^2(-i\xi)^4 \widetilde{\overline{w}} + s^2 \widetilde{\overline{w}} = s\tilde{f}(\xi) \rightarrow (k^2\xi^4 + s^2)\widetilde{\overline{w}} = s\tilde{f}(\xi) \tag{27}$$

As we try to do with any differential equation, the original fourth order partial differential equation has been reduced down to a very simple algebraic equation. Solving for $\widetilde{\overline{w}}$ in equation (27) yields

$$\widetilde{\overline{w}} = \frac{s\tilde{f}(\xi)}{(k^2\xi^4 + s^2)} \tag{28}$$

In order to determine the displacement in the correct domain, the inverse Laplace transform and inverse Fourier transform must be used. From the table of inverse Laplace transforms, it is known that $\mathcal{L}^{-1}\left[\frac{s}{\omega^2+s^2}\right] = cos(\omega t)$, thus for equation (28) we can conclude that

$$\widetilde{w} = \mathcal{L}^{-1}\left[\frac{s\tilde{f}(\xi)}{(k^2\xi^4 + s^2)}\right] = \tilde{f}(\xi)\cos(\xi^2 kt) \tag{29}$$

Finally, taking the inverse Fourier transform of equation (29) gives

$$w(x,t) = \frac{1}{2\pi}\int_{-\infty}^{\infty} \tilde{f}(\xi)\cos(\xi^2 kt)\, e^{i\xi x} d\xi \tag{30}$$

It is important to note that we could stop at this point and numerically solve the inverse Fourier transform. For the other beam theories, we will explore the method of numerically integrating equation (30) using MATLAB.

Using the convolution property, $\mathcal{F}^{-1}[\tilde{f}(\xi)\tilde{g}(\xi)] = \int_{-\infty}^{\infty} f(x-\alpha)\, g(\alpha) d\alpha$, equation (30) is rewritten as

$$w(x,t) = \frac{1}{2\pi}\int_{-\infty}^{\infty} f(x-\alpha)\mathcal{F}^{-1}\{\cos(\xi^2 kt)\}_\alpha \, d\alpha \tag{31}$$

Let's do some side work and determine what $\mathcal{F}^{-1}\{\cos(\xi^2 kt)\}_\alpha d\alpha$ is. We want to find a function, $g(x,t)$ whose Fourier transform is $\tilde{g}(\xi,t) = \cos(\xi^2 kt)$.

$$\begin{aligned}\mathcal{F}^{-1}\{\cos(\xi^2 kt)\}_\alpha &= \frac{1}{2\pi}\int_{-\infty}^{\infty} \cos(\xi^2 kt)\, e^{i\xi\alpha} d\xi \\ &= \frac{1}{2\sqrt{2\pi kt}}\left[\cos\frac{\alpha^2}{4kt} + \sin\frac{\alpha^2}{4kt}\right] = \frac{1}{2\sqrt{\pi kt}}\cos\left(\frac{\alpha^2}{4kt} - \frac{\pi}{4}\right)\end{aligned} \tag{32}$$

Combining equation (31) and (32) brings us to

$$w(x,t) = \frac{1}{2\sqrt{\pi k t}} \int_{-\infty}^{\infty} f(x-\alpha) \cos\left(\frac{\alpha^2}{4kt} - \frac{\pi}{4}\right) d\alpha \tag{33}$$

We can choose a particular initial displacement function, $f(x-\alpha)$ that will allow one to solve integral. Let $w(x,0) = f(x) = f_0 e^{-x^2/4\beta^2}$. Using this as the initial displacement, the analytical solution is obtained (Sadd).

$$w(x,t) = \frac{f_0 e^{-\frac{x^2\beta^2}{4(\beta^4+k^2t^2)}}}{\left(1+\frac{k^2t^2}{\beta^2}\right)^{1/4}} \cos\left[\frac{ktx^2}{4(\beta^4+k^2t^2)} - \frac{1}{2}\arctan\left(\frac{kt}{\beta^2}\right)\right] \tag{34}$$

3.2 Rayleigh Beam Solution

Looking back to equation (11) and combining the constants in a similar way as the Euler Bernoulli beam, we will begin with the equation

$$k^2 \frac{\partial^4 w}{\partial x^4} - b^2 \frac{\partial^4 w}{\partial x^2 \partial t^2} + \frac{\partial^2 w}{\partial t^2} = 0 \tag{35}$$

Here, $k^2 = EI/\rho A$ and $b^2 = I/A$. Similar to the Euler-Bernoulli beam, we will take the Laplace transform with respect to time with $\mathcal{L}(w) = \overline{w}(x,s)$.

$$\begin{aligned} k^2 \frac{\partial^4 \overline{w}}{\partial x^4} - b^2 \left[s\left(s\frac{\partial^2 \overline{w}}{\partial x^2} - \frac{\partial^2 w}{\partial x^2}(x,0)\right) - \frac{\partial^3 w}{\partial x^2 \partial t}(x,0)\right] ... \\ ... + s\big(s\overline{w} - w(x,0)\big) - \dot{w}(x,0) = 0 \end{aligned} \tag{36}$$

Note that if $w(x,0) = f(x)$, then $\frac{\partial^2 w}{\partial x^2} = f''(x)$. It is also specified that the initial velocity is zero, that is, $\dot{w}(x,0) = 0$. Thus we can see that $\frac{\partial^3 w}{\partial x^2 \partial t} = \dot{w}''(x,0) = 0$ and the simplifications results in

$$k^2 \frac{\partial^4 \overline{w}}{\partial x^4} - b^2 s^2 \frac{\partial^2 \overline{w}}{\partial x^2} + s^2 \overline{w} + b^2 s f''(x) - s f(x) = 0 \tag{37}$$

Now taking the Fourier transform with respect to position, and defining $\mathcal{F}(\bar{w}) = \tilde{\bar{w}}(\xi, s)$, equation (37) becomes

$$k^2(-i\xi)^4\tilde{\bar{w}} - b^2s^2(-i\xi)^2\tilde{\bar{w}} + s^2\tilde{\bar{w}} = -b^2s\tilde{f}''(\xi) + s\tilde{f}(\xi) \tag{38}$$

$$(k^2\xi^4 + b^2s^2\xi^2 + s^2)\tilde{\bar{w}} = -b^2s\tilde{f}''(\xi) + s\tilde{f}(\xi) \tag{39}$$

Again, the original fourth order partial differential equation has been reduced down to a simple algebraic equation. Solving equation (39) yields

$$\tilde{\bar{w}} = \left[-b^2\tilde{f}''(\xi) + \tilde{f}(\xi)\right]\frac{s}{(k^2\xi^4 + (b^2\xi^2 + 1)s)} \tag{40}$$

First, the inverse Laplace transform is taken. From the tables of inverse Laplace transforms, it is known that $\mathcal{L}^{-1}\left[\frac{s}{\omega^2 + xs^2}\right] = \frac{1}{x}\cos\left(\frac{1}{\sqrt{x}}\omega t\right)$. This results in

$$\tilde{w} = \mathcal{L}^{-1}\left[\frac{\left(-b^2\tilde{f}''(\xi) + \tilde{f}(\xi)\right)s}{(k^2\xi^4 + (b^2\xi^2 + 1)s)}\right] = \frac{-b^2\tilde{f}''(\xi) + \tilde{f}(\xi)}{b^2\xi^2 + 1}\cos\left(\frac{\xi^2 kt}{\sqrt{b^2\xi^2 + 1}}\right) \tag{41}$$

Unlike the Euler-Bernoulli beam, the inverse Fourier transform of equation (41) is not readily known. Instead, numerical integration will be used to approximate the inverse Fourier transform. Writing out the definition of the inverse Fourier transform, the integral that needs to be numerically solved is

$$\begin{gathered} w = \frac{1}{2\pi}\int_{-\infty}^{\infty}\tilde{w}e^{i\xi x}d\xi \\ w = \frac{1}{2\pi}\int_{-\infty}^{\infty}\left[\frac{-b^2\tilde{f}''(\xi) + \tilde{f}(\xi)}{b^2\xi^2 + 1}\cos\left(\frac{\xi^2 kt}{\sqrt{b^2\xi^2 + 1}}\right)\right]e^{i\xi x}d\xi \end{gathered} \tag{42}$$

In order to approximate the inverse Fourier transform, the improper integral is approximated as a proper integral with finite limits of integration.

$$w \approx \frac{1}{2\pi} \int_{-N}^{N} \left[\frac{-b^2 \tilde{f}''(\xi) + \tilde{f}(\xi)}{b^2 \xi^2 + 1} \cos\left(\frac{\xi^2 kt}{\sqrt{b^2 \xi^2 + 1}} \right) \right] e^{i\xi x} d\xi \tag{43}$$

Here, N represents a positive integer that is arbitrarily selected and increased until convergence in the solution is shown. Due to the complexity of the integrand, the trapezoidal method is used to numerically approximate the integral using spatial discretization.

3.3 Timoshenko Beam Solution

The solution process for the Timoshenko beam will be slightly different from the past two beam theories. Due to the fourth order derivative with respect to time, the Laplace transform causes more problems than it solves. So instead of reducing the fourth order partial differential equation down to an algebraic equation, only the Fourier transform will be used in order to reduce the partial differential equation down to a manageable, ordinary differential equation.

Starting with equation (24), let $a^2 = \frac{\rho I}{G A_s}$, $b^2 = \frac{I}{A} + \frac{EI}{G A_s}$ and $k^2 = \frac{EI}{\rho A}$.

$$a^2 \frac{\partial^4 w}{\partial t^4} - b^2 \frac{\partial^4 w}{\partial x^2 \partial t^2} + k^2 \frac{\partial^4 w}{\partial x^4} + \frac{\partial^2 w}{\partial t^2} = 0 \tag{44}$$

To begin solving equation (44), take the Fourier transform with respect to position, letting $\mathcal{F}(w) = \widetilde{w} = \widetilde{w}(\xi, t)$.

$$a^2 \frac{\partial^4 \widetilde{w}}{\partial t^4} - b^2 (-i\xi)^2 \frac{\partial^2 \widetilde{w}}{\partial t^2} + k^2 (-i\xi)^4 \widetilde{w} + \frac{\partial^2 \widetilde{w}}{\partial t^2} = 0 \tag{45}$$

Simplifying and combing like terms brings results in the ordinary differential equation.

$$a^2\frac{\partial^4\widetilde{w}}{\partial t^4}+(b^2\xi^2+1)\frac{\partial^2\widetilde{w}}{\partial t^2}+k^2\xi^4\widetilde{w}=0 \tag{46}$$

This ordinary differential equation can be solved by hand, however due to the form of the solution, it is very difficult. Instead, MATLAB can solve this ordinary differential equation, symbolically, and allows for inputting the initial conditions to solve for the unknown coefficients. With the initial conditions of $\widetilde{w}(\xi,0)=\tilde{f}(\xi)$ and $\dot{\widetilde{w}}(\xi,0)=\ddot{\widetilde{w}}(\xi,0)=\dddot{\widetilde{w}}(\xi,0)=0$, the solution takes the form

$$\widetilde{w}(\xi,t)=\frac{C_3e^{t\sqrt{-\frac{C_1}{2a^2}}}}{4C_4}+\frac{C_3e^{-t\sqrt{-\frac{C_1}{2a^2}}}}{4C_4}-\frac{e^{C_2}\tilde{f}(\xi)C_1}{4C_4}-\frac{e^{-C_2}\tilde{f}(\xi)C_1}{4C_4} \tag{47}$$

$$C_1=b^2\xi^2-C_4+1 \qquad C_2=t\sqrt{-\frac{b^2\,\xi^2\,+C_4+1}{2a^2}}$$

$$C_3=\tilde{f}(\xi)+C_4f(\xi)+b^2\xi^2f(\xi) \qquad C_4=\sqrt{(b^2\xi^2-2ak\xi^2+1)(b^2\xi^2+2ak\xi^2+1)}$$

With the Fourier transformed solution, the solution, $w(x,t)$, can be numerically integrated. By substituting equation (47) into equation (48), we obtain the solution.

$$w=\frac{1}{2\pi}\int_{-\infty}^{\infty}\widetilde{w}e^{i\xi x}d\xi\approx\frac{1}{2\pi}\int_{-N}^{N}\widetilde{w}e^{i\xi x}d\xi \tag{48}$$

Using the same method shown for the Rayleigh beam, the inverse Fourier transform can be numerically approximated. It is important to understand that in order to set up this integral, the Fourier transform of the initial condition must be known. For the same initial condition used in the Euler-Bernoulli analytical solution, the Fourier transform of the function is

$$\tilde{f}(\xi)=\mathcal{F}\big(f(x)\big)=\mathcal{F}\left(f_0e^{-\frac{x^2}{4\beta^2}}\right)=2\beta f_0\sqrt{\pi}e^{-\beta^2\xi^2} \tag{49}$$

4 SEPARATION OF VARIABLES

The separation of variables is a very well-known method used to solve partial differential equations. The method of separation of variables is described in detail in *Applied Partial Differential Equations* by Richard Haberman (Haberman). The basic idea is to assume the solution to a partial differential equation with two field variables would take the form

$$w(x,t) = X(x)T(t) \tag{50}$$

The right hand side of equation (50) is known as the separated solution and consists of the product of two, more easily obtainable, one-dimensional functions.

4.1 Euler-Bernoulli Beam

Let's begin the method of separation of variables by plugging equation (50) into the Euler-Bernoulli beam equation (25).

$$k^2 \frac{\partial^4 w}{\partial x^4} + \frac{\partial^2 w}{\partial t^2} = 0 \rightarrow k^2 T(t) \frac{d^4 X(x)}{dx^4} + X(x) \frac{d^2 T(t)}{dt^2} = 0 \tag{51}$$

Dividing equation (51) by $X(x)T(t)$ and moving one of the terms to the right hand side allows separation of the spatial variables from the temporal variables.

$$-\frac{k^2}{X(x)} \frac{d^4 X(x)}{dx^4} = \frac{1}{T(t)} \frac{d^2 T(t)}{dt^2} = -\gamma^2 \tag{52}$$

Here, γ is a separation constant (Haberman). Note that equation (52) is actually two ordinary differential equations. Moving the terms around, the two equations are

$$\frac{d^4 X}{dx^4} - \frac{\gamma^2}{k^2} X = 0 \tag{53}$$

$$\frac{d^2 T}{dt^2} + \gamma^2 T = 0 \tag{54}$$

The ordinary differential equations have well known solutions that take the form

$$X(x) = A_1 \sin\left(\sqrt{\frac{\gamma}{k}}x\right) + A_2 \cos\left(\sqrt{\frac{\gamma}{k}}x\right) + A_3 \sinh\left(\sqrt{\frac{\gamma}{k}}x\right) + A_4 \cosh\left(\sqrt{\frac{\gamma}{k}}x\right) \quad (55)$$

$$T(t) = A_5 \sin(\gamma t) + A_6 \cos(\gamma t) \quad (56)$$

Here, $A_1 - A_6$ are constants that must be solved for using the boundary conditions and initial conditions for each specific problem. For a beam with pinned boundary conditions, the moment and the displacement at each end of the beam must be zero.

$$w(0,t) = w(L,t) = 0 \quad (57)$$

$$\frac{\partial^2 w}{\partial x^2}(0,t) = \frac{\partial^2 w}{\partial x^2}(L,t) = 0 \quad (58)$$

Substituting the boundary conditions at $x = 0$ into equation (55) show that

$$X(0) = 0 = A_2 + A_4$$

$$\frac{d^2X}{dx^2}(0) = 0 = -A_2 + A_4$$

This system of equations can quickly be solved to show that $A_2 = A_4 = 0$. Then, applying the boundary condition at $x = L$ results in

$$\begin{aligned} X(L) = 0 &= A_1 \sin\left(\sqrt{\frac{\gamma}{k}}L\right) + A_3 \sinh\left(\sqrt{\frac{\gamma}{k}}L\right) \\ X(L) = 0 &= -A_1 \sin\left(\sqrt{\frac{\gamma}{k}}L\right) + A_3 \sinh\left(\sqrt{\frac{\gamma}{k}}L\right) \end{aligned} \quad (59)$$

In order for this system of equations to have a non-trivial solution, the determinant of the system must be zero.

$$2A_1A_3 \sin\left(\sqrt{\frac{\gamma}{k}}L\right) \sinh\left(\sqrt{\frac{\gamma}{k}}L\right) = 0 \quad (60)$$

In order for equation (60) to equal zero and give a non-trivial solution, either $\sin\left(\sqrt{\frac{\gamma}{k}}L\right) = 0$ or $\sinh\left(\sqrt{\frac{\gamma}{k}}L\right) = 0$. $\sinh\left(\sqrt{\frac{\gamma}{k}}L\right)$ will only equal zero if the expression within the parenthesis is zero. This would imply that $\gamma = 0$ and therefore gives the trivial solution. Thus $\sin\left(\sqrt{\frac{\gamma}{k}}L\right)$ must equal zero, or $\sqrt{\frac{\gamma}{k}}L = n\pi$ for $n = 1, 2, 3, \dots, \infty$. This can be re-written to solve for the frequencies of vibration.

$$\gamma = \frac{n^2\pi^2}{L^2}k = \frac{n^2\pi^2}{L^2}\sqrt{\frac{EI}{\rho A}} \tag{61}$$

Since it has been shown that $\sin\left(\sqrt{\frac{\gamma}{k}}L\right) = 0$, it is shown that $A_3 = 0$ for equation (59) to be true. With this known, the separated solutions are combined to give the final displacement function to be

$$w(x,t) = \sum_{n=1}^{\infty} \sin\left(\frac{n\pi x}{L}\right)[A_n \sin(\gamma_n t) + B_n \cos(\gamma_n t)] \tag{62}$$

Here, A_n and B_n are both coefficients that are determined from the initial conditions. Let us use the same initial conditions used in the Fourier transform method.

$$w(x,0) = f(x) = f_0 e^{-x^2/4\beta^2} \tag{63}$$

$$\dot{w}(x,0) = 0 \tag{64}$$

Equation (64) results in $A_n = 0$. Using equation (63) will require the use of the orthogonality relationship (Haberman). Let substitute equation (63) into equation (62)

$$w(x,0) = f(x) = \sum_{n=1}^{\infty} B_n \sin\left(\frac{n\pi x}{L}\right) \tag{65}$$

The method for deriving the orthogonality relationship is to recognize certain properties of trigonometric functions. Let's start by multiply both sides of equation (65) by $\sin\left(\frac{m\pi x}{L}\right)$ and integrate over the domain of the beam.

$$\int_0^L f(x)\sin\left(\frac{m\pi x}{L}\right)dx = \int_0^L \sum_{n=1}^{\infty} B_n \sin\left(\frac{n\pi x}{L}\right)\sin\left(\frac{m\pi x}{L}\right)dx \tag{66}$$

For all $n \neq m$, the integral on the right will evaluate to zero. Thus, the infinite series simplifies down to a single term.

$$\int_0^L f(x)\sin\left(\frac{m\pi x}{L}\right)dx = \int_0^L B_m \sin^2\left(\frac{m\pi x}{L}\right)dx \tag{67}$$

Simplifying, the final constant can be solved as

$$B_m = \frac{2}{L}\int_0^L f(x)\sin\left(\frac{m\pi x}{L}\right)dx \tag{68}$$

Knowing all the constants of integration, the final form of the solution to the original partial differential equation is

$$w(x,t) = \frac{2}{L}\sum_{n=1}^{\infty} \sin\left(\frac{n\pi x}{L}\right)\cos\left(\frac{n^2\pi^2}{L^2}bt\right)\int_0^L f(x)\sin\left(\frac{n\pi x}{L}\right)dx \tag{69}$$

4.2 Rayleigh Beam

The method of separation of variables for the Rayleigh beam is very similar to what was just used for the Euler-Bernoulli beam. Let's begin the Rayleigh beam solution by plugging equation (50) into the Euler-Bernoulli beam equation (35).

$$k^2T(t)\frac{d^4X(x)}{dx^4} - b^2\frac{d^2X(x)}{dx^2}\frac{d^2T(t)}{dt^2} + X(x)\frac{d^2T(t)}{dt^2} = 0 \tag{70}$$

By factoring out the $\frac{d^2T(t)}{dt^2}$ term, the equation can be re-written in a more useful form.

$$k^2 T \frac{d^4 X}{dx^4} = \frac{d^2 T}{dt^2}\left(b^2 \frac{d^2 X}{dx^2} - X\right) \tag{71}$$

Finally, grouping together the spatial terms on the rights side and the temporal terms on the left, the original partial differential equation has been reduced to an ordinary differential equation.

$$\frac{k^2 \frac{d^4 X}{dx^4}}{b^2 \frac{d^2 X}{dx^2} - X} = \frac{\frac{d^2 T}{dt^2}}{T} = -\gamma^2 \tag{72}$$

Here, γ is the separation constant. The temporal ordinary differential equation is exactly the same as that of the Euler-Bernoulli beam. The solution to the spatial portion is slightly different. Let's assume the solution takes the from $X(x) = Ae^{rx}$. Substituting into the differential equation yields the following characteristic equation.

$$r^4 + \frac{\gamma^2 b^2}{k^2} r^2 - \frac{\gamma^2}{b^2} = 0 \tag{73}$$

The four roots to this equation are

$$r_{1,2} = \pm \sqrt{\frac{-\gamma^2 b^2}{2k^2} - \sqrt{\frac{\gamma^4 b^4}{4k^4} + \frac{\gamma^2}{k^2}}} \tag{74}$$

$$r_{3,4} = \pm \sqrt{\frac{-\gamma^2 b^2}{2k^2} + \sqrt{\frac{\gamma^4 b^4}{4k^4} + \frac{\gamma^2}{k^2}}} \tag{75}$$

With these roots, the spatial separated solution takes the form

$$X(x) = A_1 e^{r_1 t} + A_2 e^{r_2 t} + A_3 e^{r_3 t} + A_4 e^{r_4 t} \tag{76}$$

Now, recognize that if $r_{1,2} = \pm im_1$ and $r_{3,4} = \pm m_2$, equation (76) can be transformed into a much more useful form.

$$X(x) = A_1 \sin(m_1 x) + A_2 \cos(m_1 x) + A_3 \sinh(m_2 x) + A_4 \cosh(m_2 x) \qquad (77)$$

This form of the solution is much more useful as the boundary conditions will allow one to easily solve for the constants of integration. Using equation (57) and equation (58) as the boundary conditions for a beam with both ends pinned, it is shown that $A_2 = 0$ and $A_4 = 0$, just as in the Euler-Bernoulli solution. Using the boundary condition at $x = L$ will yield $\sin(m_n L) = 0$ for the non-trivial solution. The sine function equals zero when the input is a constant multiple of π, that is

$$m_n L = n\pi \rightarrow m_n = \frac{n\pi}{L} \qquad (78)$$

With the knowledge of m_n, the value of the frequency, γ can be determined as

$$r_1 = \sqrt{\frac{-\gamma^2 b^2}{2k^2} - \sqrt{\frac{\gamma^4 b^4}{4k^4} + \frac{\gamma^2}{k^2}}} = im_n = \frac{in\pi}{L} \qquad (79)$$

Solving for γ gives

$$\gamma_{1,2} = \pm \frac{\pi^2 k n^2}{\sqrt{\pi^2 b^2 L^2 n^2 + L^4}} \qquad (80)$$

Note that due to how γ was initially defined, the negative value of γ would result in a trivial solution. Thus, we know that the positive value must be used. Using the orthogonality relationship, exactly as we did in the Euler-Bernoulli solution, the final solution for the Rayleigh beam is

$$w(x,t) = \frac{2}{L} \sum_{n=1}^{\infty} \sin\left(\frac{n\pi x}{L}\right) \cos\left(\frac{\pi^2 k n^2}{\sqrt{\pi^2 b^2 L^2 n^2 + L^4}} t\right) \int_0^L f(x) \sin\left(\frac{n\pi x}{L}\right) dx \qquad (81)$$

Let's take note that the only difference in the Rayleigh beam and the Euler-Bernoulli beam is the frequency. We will see this same result when solving the Timoshenko beam using the separation of variables.

4.3 Timoshenko Beam

To solve the Timoshenko beam, we will need to take a slightly different approach from the last two. However it will start by plugging equation (50) into the Timoshenko beam equation (24). Note that $b^2 = \frac{I}{A}$, $k^2 = \frac{EI}{\rho A}$ and $d^2 = \frac{\rho\kappa}{G}$. κ is the shear area correction factor, such that $A_s = A/\kappa$.

$$\begin{gathered} b^2d^2\frac{d^4w}{dt^4} - (b^2 + k^2d^2)\frac{d^4w}{dx^2dt^2} + k^2\frac{d^4w}{dx^4} + \frac{d^2w}{dt^2} = 0 \\ b^2d^2X\frac{d^4T}{dt^4} - (b^2 + k^2d^2)\frac{d^2T}{dt^2}\frac{d^2X}{dx^2} + k^2T\frac{d^4X}{dx^4} + \frac{Xd^2T}{dt^2} = 0 \end{gathered} \tag{82}$$

Dividing equation (82) by the separated solution, $X(x)T(t)$, a more useful form is obtained.

$$\frac{b^2d^2}{T}\frac{d^4T}{dt^4} - \frac{(b^2 + k^2d^2)}{XT}\frac{d^2T}{dt^2}\frac{d^2X}{dx^2} + \frac{k^2}{X}\frac{d^4X}{dx^4} + \frac{1}{T}\frac{d^2T}{dt^2} = 0 \tag{83}$$

At this point, it is recognized that the equation is not readily separable into the spatial and temporal sides. However, a useful trick when this happens is to take the derivative of the whole equation with respect to one of the field variables. In this case, let's take the derivative of equation (83) with respect to the spatial variable (Harrevelt).

$$\begin{gathered} \frac{d}{dx}\left(\frac{b^2d^2}{T}\frac{\partial^4T}{\partial t^4} - \frac{(b^2 + k^2d^2)}{XT}\frac{d^2T}{dt^2}\frac{d^2X}{dx^2} + \frac{k^2}{X}\frac{d^4X}{dx^4} + \frac{1}{T}\frac{d^2T}{dt^2} = 0\right) \\ \frac{d}{dx}\left(\frac{k^2}{X}\frac{d^4X}{dx^4}\right) - \frac{d}{dx}\left(\frac{(b^2 + k^2d^2)}{X}\frac{d^2X}{dx^2}\right)\frac{d^2T}{dt^2}\frac{1}{T} = 0 \end{gathered} \tag{84}$$

Now, equation (84) can be separated into the spatial and temporal components.

$$\frac{\frac{d}{dx}\left(\frac{k^2}{X}\frac{d^4X}{dx^4}\right)}{\frac{d}{dx}\left(\frac{(b^2+k^2d^2)}{X}\frac{d^2X}{dx^2}\right)} = \frac{d^2T}{dt^2}\frac{1}{T} = -\gamma^2 \tag{85}$$

Although the spatial component of equation (85) looks daunting, only the temporal component is needed at this time. Again, the solution for the temporal component is exactly the same as that of the Euler-Bernoulli solution and the Rayleigh solution.

$$T(t) = A_5 \sin(\gamma t) + A_6 \cos(\gamma t) \tag{86}$$

Before moving onto the solution to the spatial component, let's take note that

$$\begin{gathered} \frac{d^2T}{dt^2} = -\gamma^2 T \\ \frac{d^2}{dt^2}\left(\frac{d^2T}{dt^2} = -\gamma^2 T\right) \rightarrow \frac{d^4T}{dt^4} = -\gamma^2\frac{d^2T}{dt^2} \rightarrow \frac{d^4T}{dt^4} = \gamma^4 T \end{gathered} \tag{87}$$

Substituting equation (87) into equation (83), the partial differential equation reduces to an ordinary differential equation.

$$b^2d^2\gamma^4 + \frac{(b^2+k^2d^2)\gamma^2}{X}\frac{d^2X}{dx^2} + \frac{k^2}{X}\frac{d^4X}{dx^4} - \gamma^2 = 0 \tag{88}$$

Multiplying through by $X(x)$ results in a more useful form.

$$k^2\frac{d^4X}{dx^4} + (b^2+k^2d^2)\gamma^2\frac{d^2X}{dx^2} - \gamma^2X(1-b^2d^2\gamma^2) = 0 \tag{89}$$

By assuming the solution takes the form $X(x) = Ae^{rt}$, we can obtain a characteristic equation whose roots are

$$r_{1,2} = \pm\sqrt{-\frac{b^2\gamma^2 - \gamma\sqrt{b^4\gamma^2 - 2b^2d^2\gamma^2k^2 + d^4\gamma^2k^4 + 4k^2} + d^2\gamma^2k^2}{2k^2}} \tag{90}$$

$$r_{3,4} = \pm\sqrt{-\frac{b^2\gamma^2 + \gamma\sqrt{b^4\gamma^2 - 2b^2d^2\gamma^2k^2 + d^4\gamma^2k^4 + 4k^2} + d^2\gamma^2k^2}{2k^2}} \tag{91}$$

Again, recognize that if $r_{1,2} = \pm im_1$ and $r_{3,4} = \pm m_2$, the solution is written in a sinusoidal form.

$$X(x) = A_1\sin(m_1x) + A_2\cos(m_1x) + A_3\sinh(m_2x) + A_4\cosh(m_2x) \tag{92}$$

The process for solving for the unknown constants is exactly the same as the previous two solutions. For the pinned beam, $A_2 = A_4 = A_3 = 0$ and $m_1 = n\pi/L$. Thus we can back out what γ is.

$$r_1 = im_n$$

$$\sqrt{-\frac{b^2\gamma^2 - \gamma\sqrt{b^4\gamma^2 - 2b^2d^2\gamma^2k^2 + d^4\gamma^2k^4 + 4k^2} + d^2\gamma^2k^2}{2k^2}} = \frac{in\pi}{L} \tag{93}$$

Solving for γ gives

$$\gamma = \left[-\frac{\sqrt{(-\pi^2b^2L^2n^2 - \pi^2d^2k^2L^2n^2 - L^4)^2 - 4\pi^4b^2d^2k^2L^4n^4}}{2b^2d^2L^4} + \frac{1}{2b^2d^2} + \frac{\pi^2k^2n^2}{2b^2L^2} + \frac{\pi^2n^2}{2d^2L^2}\right]^{\frac{1}{2}} \tag{94}$$

Using the orthogonality property with the initial conditions being the same as the last two solutions, the final solution to the Timoshenko beam takes the form

$$w(x,t) = \frac{2}{L}\sum_{n=1}^{\infty}\sin\left(\frac{n\pi x}{L}\right)\cos(\gamma t)\int_0^L f(x)\sin\left(\frac{n\pi x}{L}\right)dx \tag{95}$$

5 FINITE ELEMENT APPROXIMATION

5.1 Euler-Bernoulli Beam Approximation

Taking a step back to equation (7), the principle of virtual work can be implemented to approximate the solution. Multiplying equation (7) by the virtual displacement, $\bar{w}$, and integrating over the domain of the beam results in:

$$\int_0^L [EIw'''' + \rho A\ddot{w}]\bar{w}dx = 0 \tag{96}$$

The fourth order derivative can be separated using integration by parts. Two boundary terms show up, but for all standard boundary conditions, these will equal zero.

$$\int_0^L EIw''\bar{w}'' + \rho A\ddot{w}\bar{w}\,dx = 0 \tag{97}$$

Using the Rayleigh Ritz Method, the displacement and virtual displacement can be written in the form:

$$w(x,t) = \mathbf{a}^T(t)\mathbf{h}(x) \tag{98}$$

$$\bar{w}(x) = \bar{\mathbf{a}}^T\mathbf{h}(x) \tag{99}$$

Plugging in the Rayleigh Ritz approximations from equation (98) and equation (99), and factoring out, $\bar{\mathbf{a}}^T$, equation (96) becomes:

$$\bar{\mathbf{a}}^T\left[\mathbf{a}(t)\int_0^L EI\mathbf{h}''\mathbf{h}''^T\,dx + \ddot{\mathbf{a}}(t)\int_0^L \rho A\mathbf{h}\mathbf{h}^T\,dx\right] = 0 \tag{100}$$

The calculus of variation tells us that if equation (100) equals zero for any $\bar{\mathbf{a}}^T$, then the expression within the square brackets must equal zero.

$$M\ddot{\mathbf{a}}(t) + K\mathbf{a}(t) = 0 \tag{101}$$

Here $M = \int_0^L \rho A\mathbf{h}\mathbf{h}^T\,dx$ and $K = \int_0^L EI\mathbf{h}''\mathbf{h}''^T\,dx$.

5.2 Rayleigh Beam Approximation

Beginning with equation (11), let's combine the constant terms to give

$$k^2 \frac{\partial^4 w}{\partial x^4} - b^2 \frac{\partial^4 w}{\partial x^2 \partial t^2} + \frac{\partial^2 w}{\partial t^2} \tag{102}$$

Here, $k^2 = EI/\rho A$ and $b^2 = I/A$. Multiplying by the virtual displacement and integrating over the domain results in the virtual work functional

$$\int_0^L (k^2 w'' \overline{w}'' - b^2 \ddot{w}' \overline{w}' + \ddot{w} \overline{w}) dx = 0 \tag{103}$$

Similar to the Euler-Bernoulli beam, let the displacement and virtual displacement take the form of

$$w(x,t) = \mathbf{a}^T(t)\mathbf{h}(x) \tag{104}$$

$$\overline{w}(x) = \bar{\mathbf{a}}^T \mathbf{h}(x) \tag{105}$$

Plugging the new form into the virtual work functional, equation (103), and factoring out the virtual portion yields

$$\bar{\mathbf{a}}^T \left[\mathbf{a}(t) \int_0^L EI \mathbf{h}'' \mathbf{h}''^T \, dx + \ddot{\mathbf{a}}(t) \int_0^L (\rho A \mathbf{h}\mathbf{h}^T + \rho I \mathbf{h}' \mathbf{h}'^T) \, dx \right] = 0 \tag{106}$$

Again, the calculus of variations tells us that the expression within the square brackets must equal zero for equation (106) to always be true. Thus the equation of motion becomes

$$M\ddot{\mathbf{a}}(t) + K\mathbf{a}(t) = 0 \tag{107}$$

Here, $M = \int_0^L (\rho A \mathbf{h}\mathbf{h}^T + \rho I \mathbf{h}' \mathbf{h}'^T) \, dx$ and $K = \int_0^L EI \mathbf{h}'' \mathbf{h}''^T \, dx$.

5.3 Timoshenko Beam Approximation

The Timoshenko beam can best be approximated by beginning with equation (16) and equation (19). The system can be modified slightly to take the form

$$\begin{gathered}[GA_s(w'-\psi)]'-\rho A\ddot{w}=0\\ EI\psi''+GA_s(w'-\psi)-\rho I\ddot{\psi}=0\end{gathered} \tag{108}$$

Multiplying by the virtual displacement and integrating over the domain gives the virtual work functional to be

$$\int_0^L [GA_s(w'-\psi)\bar{w}'+\rho A\ddot{w}\bar{w}+EI\psi'\bar{\psi}-GA_s(w'-\psi)\bar{\psi}-\rho I\ddot{\psi}\bar{\psi}]dx \tag{109}$$

There are two boundary conditions in equation (109), however these terms integrate to zero for all standard boundary conditions. Letting the displacement and virtual displacement take the form

$$w(x,t)=\mathbf{h}^T(x)\mathbf{a}(t) \tag{110}$$

$$\bar{w}(x)=\mathbf{h}^T(x)\bar{\mathbf{a}} \tag{111}$$

$$\psi(x,t)=\mathbf{g}^T(x)\mathbf{a}(t) \tag{112}$$

$$\bar{\psi}(x)=\mathbf{g}^T(x)\bar{\mathbf{a}} \tag{113}$$

Substituting the Ritz approximations into equation (109) and factoring out the virtual terms results in (Hjelmstad)

$$\bar{\mathbf{a}}^T[\mathbf{K}_{aa}\mathbf{a}+\mathbf{K}_{ab}\mathbf{b}+\mathbf{M}_{aa}\ddot{\mathbf{a}}]+\bar{\mathbf{b}}^T\left[\mathbf{K}_{ba}\mathbf{a}+\mathbf{K}_{bb}\mathbf{b}+\mathbf{M}_{bb}\ddot{\mathbf{b}}\right]=0 \tag{114}$$

Here, $\mathbf{M}_{aa}=\int_0^L \rho A\mathbf{h}\mathbf{h}^T dx$ and $\mathbf{M}_{bb}=\int_0^L \rho I\mathbf{g}\mathbf{g}^T dx$.

The four stiffness matrices can be written out as

$$\mathbf{K}_{aa} = \int_0^L GA_s \mathbf{h}' \mathbf{h}'^T dx \qquad \mathbf{K}_{ab} = -\int_0^L GA_s \mathbf{h}' \mathbf{g}^T dx$$

$$\mathbf{K}_{ba} = -\int_0^L GA_s \mathbf{g}' \mathbf{h}^T dx \qquad \mathbf{K}_{bb} = \int_0^L EI \mathbf{g}' \mathbf{g}'^T + GA_s \mathbf{g}\mathbf{g}^T dx$$

With the mass and stiffness matrices define, the final equation of motion for the Timoshenko beam is

$$\begin{bmatrix} \mathbf{M}_{aa} & \mathbf{0} \\ \mathbf{0} & \mathbf{M}_{bb} \end{bmatrix} \begin{Bmatrix} \ddot{\mathbf{a}} \\ \ddot{\mathbf{b}} \end{Bmatrix} + \begin{bmatrix} \mathbf{K}_{aa} & \mathbf{K}_{ab} \\ \mathbf{K}_{ba} & \mathbf{K}_{bb} \end{bmatrix} \begin{Bmatrix} \mathbf{a} \\ \mathbf{b} \end{Bmatrix} = 0 \tag{115}$$

The Timoshenko beam theory still has the effects of rotary inertia within the mass matrix, however the addition of the shear term is shown by creating a system of equations, linking the shear deformation to the rotational deformation.

6 NUMERICAL INTEGRATION

In the last chapter, we saw how the finite element method can be used to put the partial differential equation into an ordinary differential equation. This left us with an equation of motion which, in general, is represented as

$$M\ddot{\mathbf{w}} + C\dot{\mathbf{w}} + K\mathbf{w} = \mathbf{f}(t) \tag{116}$$

6.1 Newmark's Method (Generalized Trapezoidal Rule)

One way to solve equation (116) is by approximating the integral with the use of the trapezoidal rule.

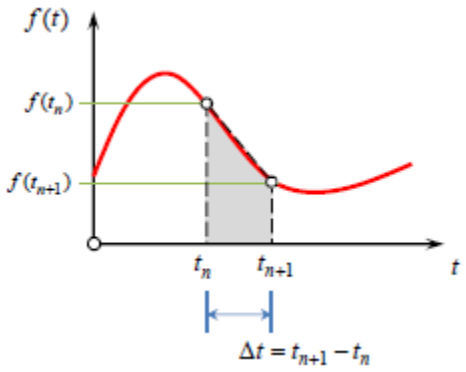

Figure 11: Visualization of the Trapezoidal Method for Numerical Integration

An integral, it its most simple definition, is the area under a curve. Knowing this fact, one could integrate a very complicated equation of motion in a very simple manor. As seen in Figure 11, a right trapezoid is used to very closely approximate the area under the curve during a time step $\Delta t = t_{n+1} - t_n$. As we shrink the time step, a better approximation will be obtained.

The area of a trapezoid is $A = \frac{1}{2}b(h_1 + h_2)$ where b would be the base of the trapezoid, in our case, $b = \Delta t$. The height of each leg corresponds to the value of the function at each time, $h_1 = f(t_n)$ and $h_2 = f(t_{n+1})$.

When given initial conditions, the value of $\mathbf{w}, \dot{\mathbf{w}}$ and $\ddot{\mathbf{w}}$ would all be known, thus only the value of the right leg of the trapezoid is all that is required. Let's recognize that the integral of the acceleration function, $\ddot{\mathbf{w}}$ is the velocity. That being said, the velocity at the next time step is written as

$$\begin{gathered}(\dot{\mathbf{w}})_{n+1} = (\dot{\mathbf{w}})_n + \Delta t[\beta(\ddot{\mathbf{w}})_n + (1-\beta)(\ddot{\mathbf{w}})_{n+1}] \\ (\dot{\mathbf{w}})_{n+1} = c_n + \Delta t(1-\beta)(\ddot{\mathbf{w}})_{n+1}\end{gathered} \tag{117}$$

Here, $\beta = \frac{1}{2}$, for the trapezoidal method. Similarly, integrating the velocity gives the position function.

$$\begin{gathered}(\mathbf{w})_{n+1} = (\mathbf{w})_n + \Delta t[\beta(\dot{\mathbf{w}})_n + (1-\beta)(\dot{\mathbf{w}})_{n+1}] \\ (\mathbf{w})_{n+1} = b_n + \Delta t^2(1-\beta)(\ddot{\mathbf{w}})_{n+1}\end{gathered} \tag{118}$$

Plugging equation (118) back into the original equation of motion, we get

$$M\ddot{\mathbf{w}}_{n+1} + C[c_n + \Delta t(1-\beta)(\ddot{\mathbf{w}})_{n+1}] + K[b_n + \Delta t^2(1-\beta)(\ddot{\mathbf{w}})_{n+1}] = 0 \tag{119}$$

This integration scheme has converted the ordinary differential equation into an algebraic equation. Once we solve for $\ddot{\mathbf{w}}_{n+1}$ at the current time step, the displacement, $(\mathbf{w})_{n+1}$ is solved using equation (118).

6.2 Fourth Order Runge-Kutta Method

The fourth order Runge-Kutta method is one of the most popular and well known methods for numerical integration. Although the computation time is greater than some other numerical integration methods, the fourth order Runge-Kutta method is widely used for the fact that the error is on the order of Δt^4 (Venkatachalam).

Looking back at equation (116), let's define two more variables.

$$\mathbf{z} = \begin{Bmatrix}\mathbf{w} \\ \dot{\mathbf{w}}\end{Bmatrix}, \dot{\mathbf{z}} = \begin{Bmatrix}\dot{\mathbf{w}} \\ \ddot{\mathbf{w}}\end{Bmatrix} \tag{120}$$

With this new definition, the equation of motion is re-written into a form that, at first, looks more complex, but will allow for easy implementation of the fourth order Runge-Kutta method.

$$\begin{bmatrix} \mathbf{I} & \mathbf{0} \\ \mathbf{0} & \mathbf{I} \end{bmatrix} \begin{Bmatrix} \dot{\mathbf{w}} \\ \ddot{\mathbf{w}} \end{Bmatrix} + \begin{bmatrix} \mathbf{0} & -\mathbf{I} \\ \mathbf{M}^{-1}\mathbf{K} & \mathbf{M}^{-1}\mathbf{C} \end{bmatrix} \begin{Bmatrix} \mathbf{w} \\ \dot{\mathbf{w}} \end{Bmatrix} - \begin{Bmatrix} \mathbf{0} \\ \mathbf{M}^{1}\mathbf{f}(t) \end{Bmatrix} = \begin{Bmatrix} \mathbf{0} \\ \mathbf{0} \end{Bmatrix}$$
$$\dot{\mathbf{z}} = \mathbf{A}\mathbf{z} - \mathbf{F}(t) = \mathbf{g}(\mathbf{z}, t) \tag{121}$$

Applying the fourth order Runge-Kutta method, the solution takes the form

$$\mathbf{z}_{n+1} = \mathbf{z}_n + \frac{1}{6}\Delta t(\mathbf{k}_1 + 2\mathbf{k}_2 + 2\mathbf{k}_3 + \mathbf{k}_4)$$
$$\mathbf{k}_1 = \mathbf{A}\mathbf{z}_n - \mathbf{F}(t_n)$$
$$\mathbf{k}_2 = \mathbf{A}\left(\mathbf{z}_n + \frac{1}{2}\Delta t\mathbf{k}_1\right) - \mathbf{F}\left(t_n + \frac{1}{2}\Delta t\right) \tag{122}$$
$$\mathbf{k}_3 = \mathbf{A}\left(\mathbf{z}_n + \frac{1}{2}\Delta t\mathbf{k}_2\right) - \mathbf{F}\left(t_n + \frac{1}{2}\Delta t\right)$$
$$\mathbf{k}_4 = \mathbf{A}(\mathbf{z}_n + \Delta t\mathbf{k}_3) - \mathbf{F}(t_n + \Delta t)$$

Going into the first time step, the initial conditions will give the knowledge of $\mathbf{z}_0$, thus allowing to solve for $\mathbf{z}_{n+1}$ at the next time purely algebraically.

7 MODELING & RESULTS

7.1 Euler-Bernoulli Beam Results

Unlike the Rayleigh beam or the Timoshenko beam, an analytical solution with a finite number of terms was achieved for the Euler-Bernoulli beam. This fact is very important because if the results of any of the numerical results match the analytical solution, then we know the numerical technique is accurate.

7.1.1 An Analytical Solution

The analytical solution for the Euler-Bernoulli beam is a single equation without any integrals that still need to be evaluated. Therefore, there are no adjustments that can be made to fine tune the plots shown in Figure 12. The first, and most important results that is noticed in Figure 12 is that the initial wave still disperses. Immediately, this shows that the transverse displacement does have a dispersive nature.

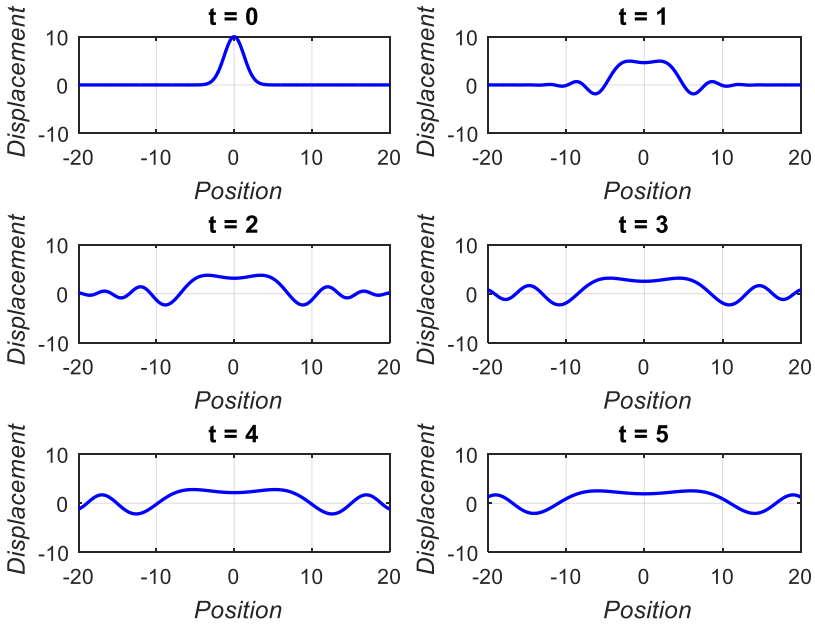

Figure 12: Euler-Bernoulli Beam - Analytical Solution

7.1.2 Fourier Analysis

Although the analytical results seem to confirm the dispersive nature, it is important to be able to verify results using multiple methods. If the waves do disperse, then the dispersion should be shown through any numerical scheme used. Looking back at equation (30), before the inverse Fourier transform is taken, numerical integration can be used to approximate the integral defined by the inverse Fourier transform. This seems counterintuitive as the analytical solution for the Euler-Bernoulli beam has already been derived, but for the other beam theories, the analytical solution was not obtained. If we can show that the numerical integration technique used to approximate the inverse Fourier transform coincides with the analytical solution for the Euler-Bernoulli beam, then when moving on to the Rayleigh beam, we will have reasoning to believe the numerical integration is accurate and the Fourier analysis on the Rayleigh beam can be verified.

Because this is a numerical integration technique, the size of the discretization will also play a role in the accuracy and precision of the solution. Figure 13 shows inaccurate results due to the coarse discretization used in the numerical integration. Figure 14 shows convergence in the solution as the step size is increased by a factor of 10. It can also be seen that the displacements shown in Figure 14 are nearly identical to the displacements shown by the analytical solution in Figure 12. This recognition helps to verify that the numerical integration used for the inverse Fourier transform can be used with confidence for the other beams models.

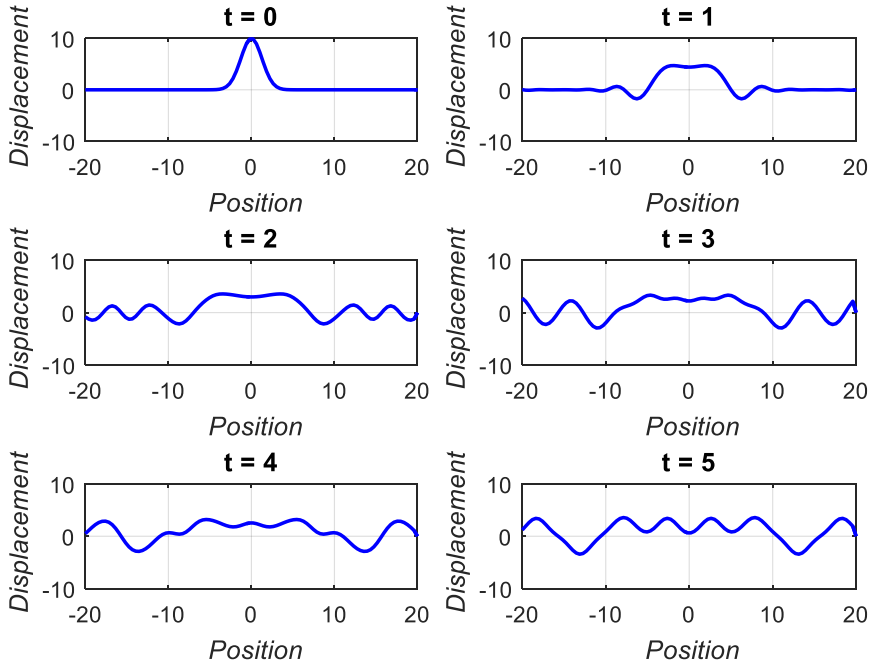

Figure 13: Inverse Fourier Transform Approximation - 0.001 Step Size

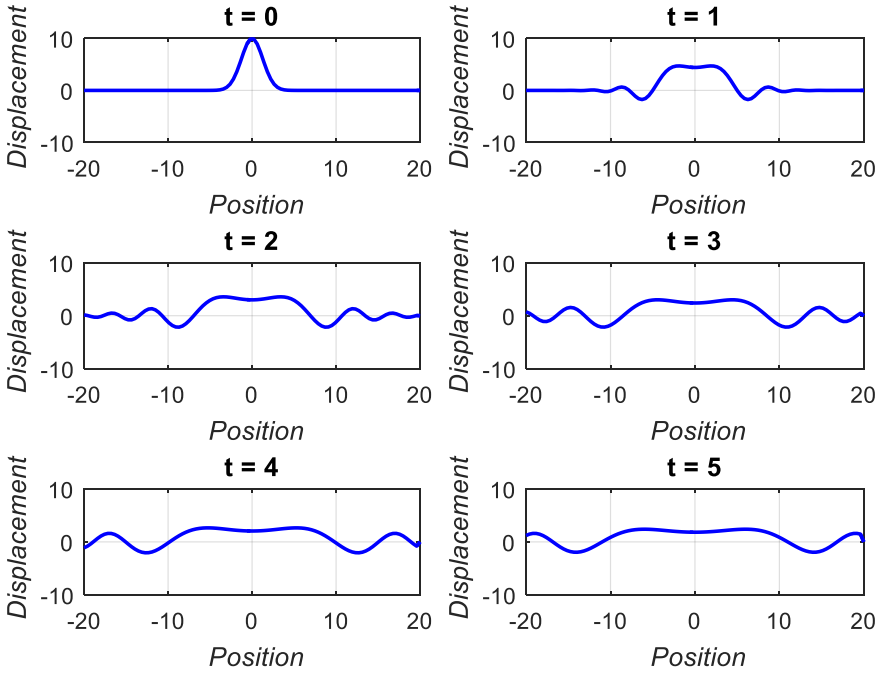

Figure 14: Inverse Fourier Transform Approximation – 0.0001 Step Size (Convergence)

7.1.3 Separation of Variables

The method of separation of variables results in a solution that requires an infinite sum. In order to model this, we will truncate the summation at a large value such that convergence is shown in the results. Using 100 terms in the series expansion, convergence can be seen in the results.

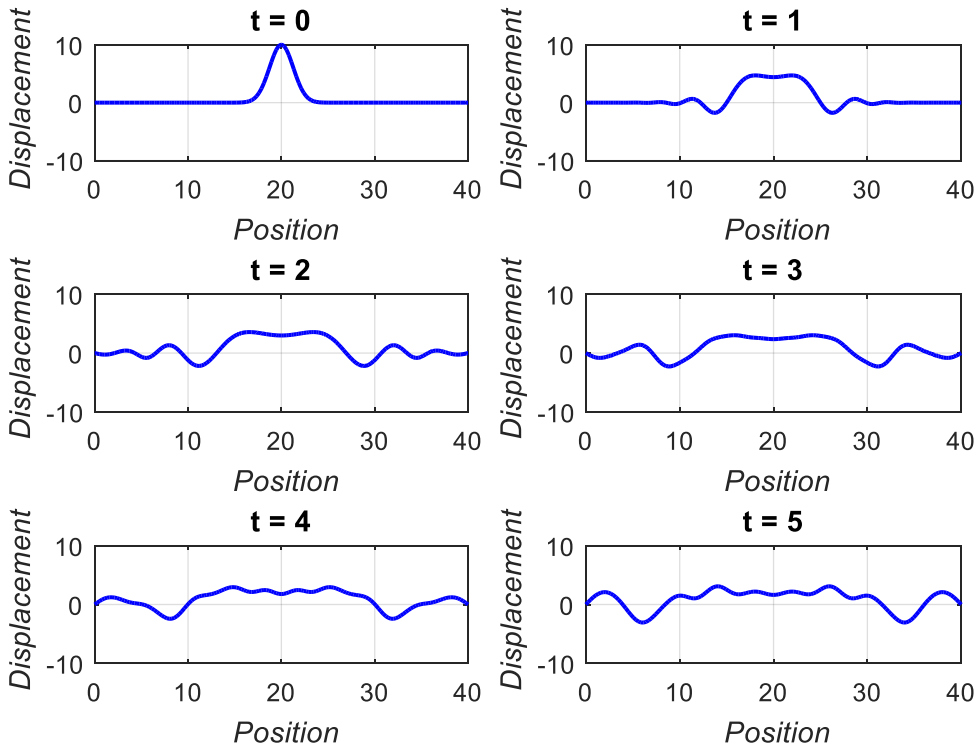

Figure 15: Separation of Variables with 200 Terms in the Series Expansion

The first few frames in Figure 15 are giving good results, however the other frames seem to be much different. The reasoning for this is entirely due to the boundary conditions. Remember that using the Fourier transform, the assumption is made that the beam is infinitely long, and thus, there are no boundaries that the waves could reflect at.

The infinitely long beam can be mimicked by using a really long beam, such that the waves do not reach the boundary by the time the analysis is complete.

Using a beam that is 200 units long, we can keep domain of the plots to stay within the 40 unit domain. Figure 16 shows great results when compared to Figure 12 and Figure 14.

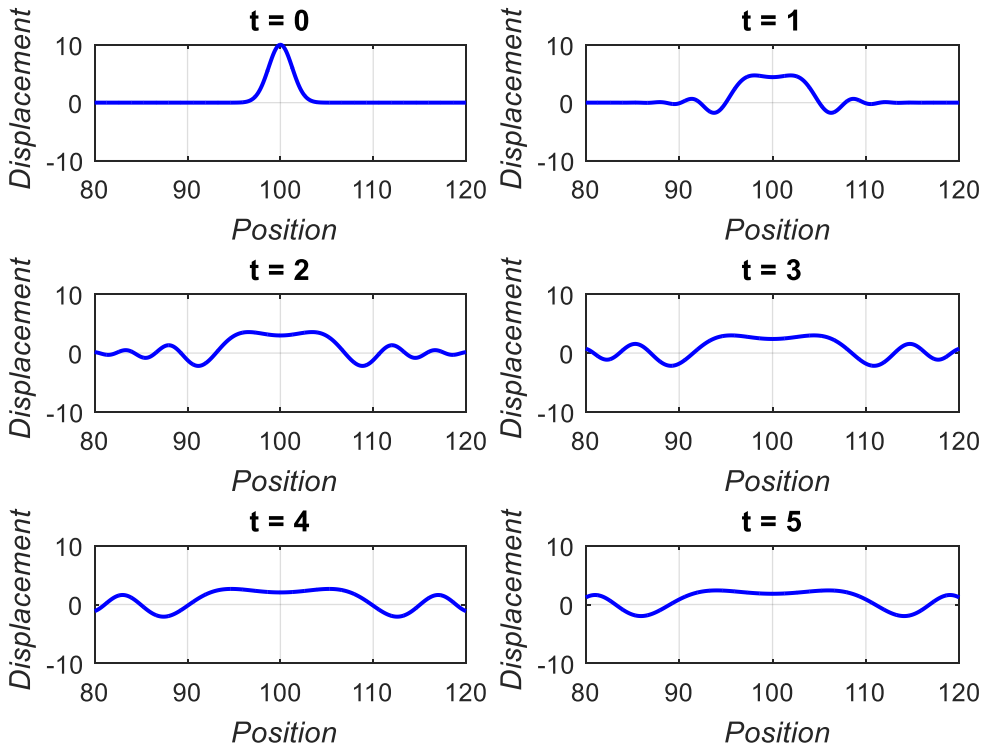

Figure 16: Separation of Variables with 200 Terms and 200 Units Long

7.1.4 Finite Element Analysis with Newmark' Method

The finite element approach also uses the effects of the boundary conditions, so we can see if those results are consistent with the separation of variables method. However, we can also mimic the infinitely long beam in the same manor used in the previous section to verify results across all methods. Figure 17 shows the displacement of

the beam with the boundary conditions considered. We can see the results very similar to the results shown in Figure 15 which suggest that we are seeing the correct results.

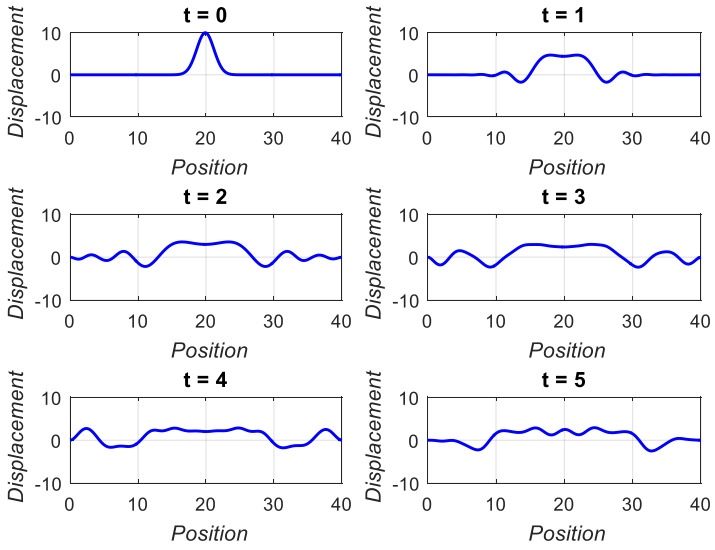

Figure 17: Finite Element Approximation – 200 Elements – 0.001 Time Step

Using a beam of 200 units in length and increasing the spatial discretization to account for the larger spatial domain, a beam with no boundaries is modeled.

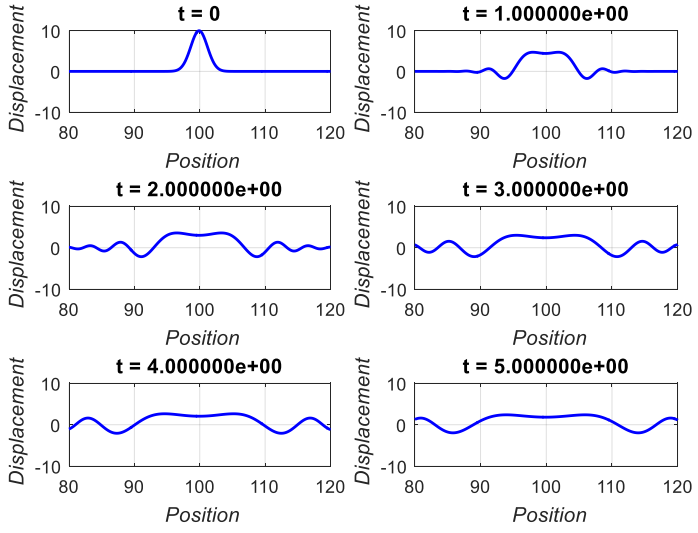

Figure 18: Finite Element - Newmark's Method – 1000 Elements – 0.001 Time Step – 200 Units Long

Figure 18 again shows the dispersion, and shows nearly identical results between the solution methods.

7.1.5 Finite Element Analysis with Fourth Order Runge-Kutta Method

The fourth order Runge-Kutta method will help to verify that there are no issues with the Newmark's approach. Again, since we are using the finite element method, the boundary conditions are considered in the results.

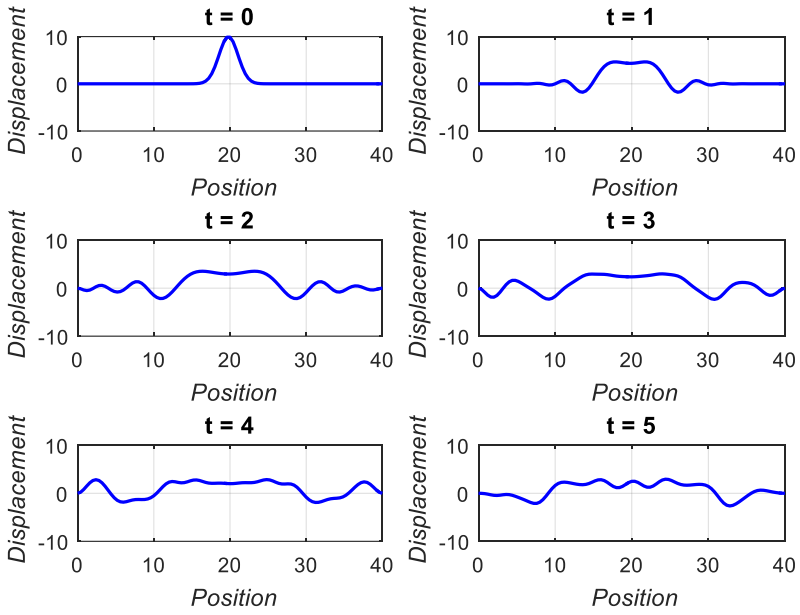

Figure 19: Finite Element - Fourth Order Runge-Kutta Method - 100 Elements - 0.001 Time Step

Comparing Figure 19 to Figure 17, we can see that the results are basically identical.

To see the results compared to the analytical solution and the Fourier transform solution, we model the beam as 200 units long to mimic the infinitely long beam. The results shown in Figure 20 are, again, basically identical to the results shown in all the other solution methods.

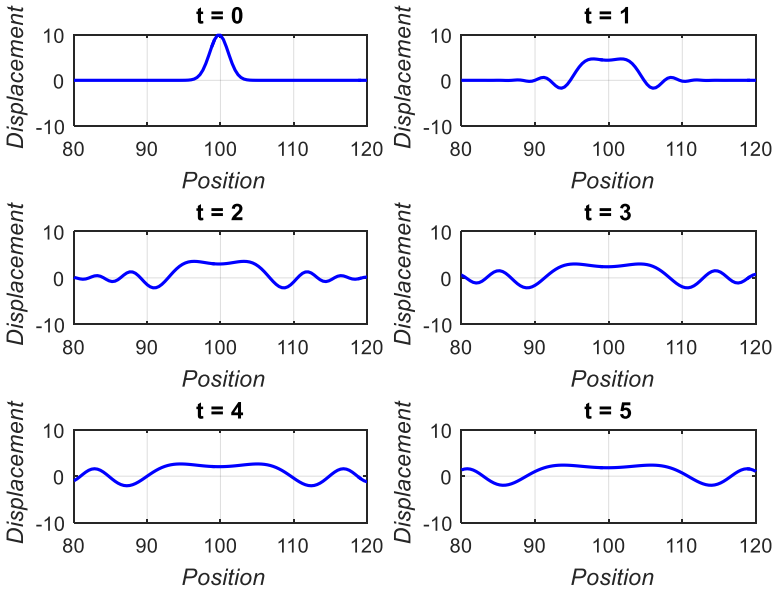

Figure 20: Finite Element - Fourth Order Runge-Kutta Method - 500 Elements - 200 Units Long

7.2 Rayleigh Beam Results

With the inclusion of the rotary motion, the shape of the displacement curve should change, yet still hold the dispersive nature shown in the Euler-Bernoulli beam. For the Rayleigh beam, an analytical solution was not acquired, but the other solution methods have shown convergence to a single solution, so there is plenty of confidence that the methods would work.

7.2.1 Fourier Analysis

Using results that have shown convergence, Figure 21 shows the dispersive nature of the Rayleigh beam. Comparing these results to Figure 14, the effects of the rotary motion can be seen. Less high frequency motion is being shown closer to the end of the beams. This is because the motion frequency has a limit as the wave number goes to infinity (Sadd). The Euler-Bernoulli beam does not have a limit, and if the wave number

goes to infinity, the frequency can go to infinity as well. This explains why high frequency vibrations are modeled better with more advanced beam theories.

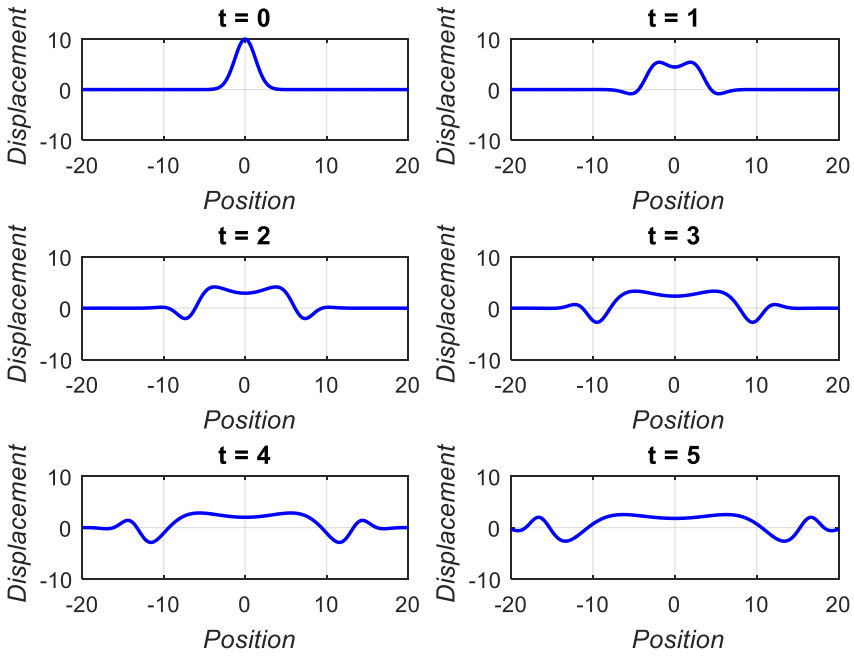

Figure 21: Rayleigh Beam - Inverse Fourier Transform Approximation

7.2.2 Separation of Variables

Using the separation of variables method, the results are shown to converge to the solution shown in Figure 21. Unlike the Euler-Bernoulli beam, we are not seeing the effects of the boundary conditions at $t = 5$ seconds.

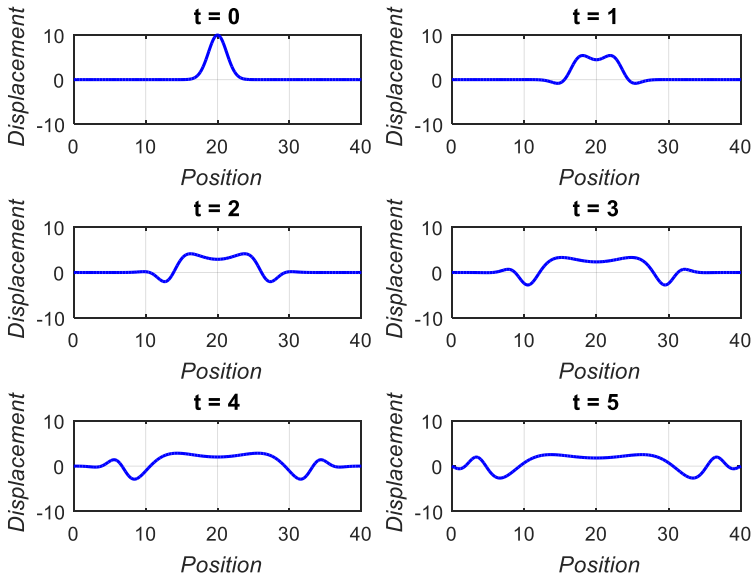

Figure 22: Rayleigh Beam – Separation of Variables – 200 Terms in Series Expansion - 40 Units Long

7.2.3 Finite Element Analysis with Newmark's Method

Using the finite element method, we see the same results from Figure 23

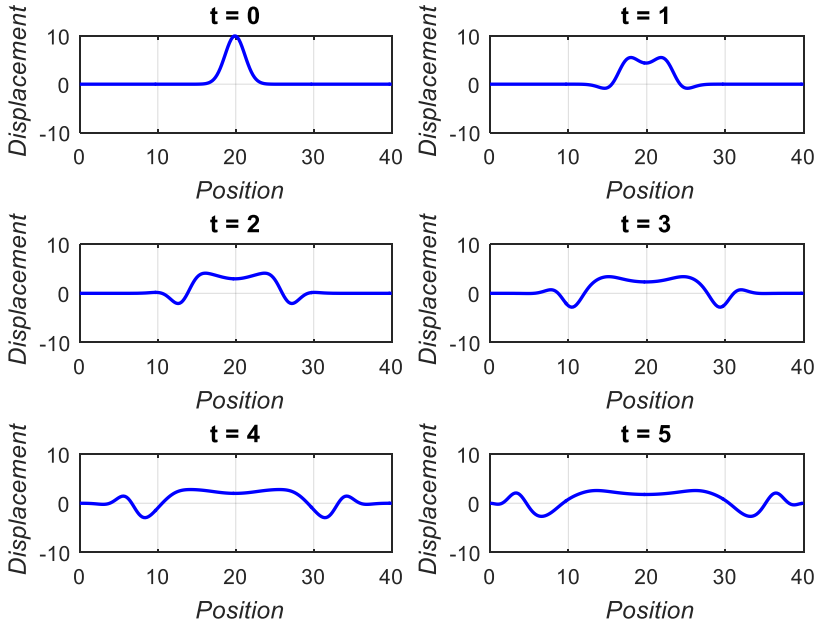

Figure 23: Rayleigh Beam - Finite Element Approximation – 200 Elements – 40 Units Long

7.2.4 Finite Element Analysis with Fourth Order Runge-Kutta Method

Using the fourth order Runge-Kutta method to perform the time integration, we still see identical results to Figure 22 and Figure 23. Overall the results across all these methods are very satisfying. The results are all based on visually observing convergence, and it is very easy to see the convergence shown across the solution methods.

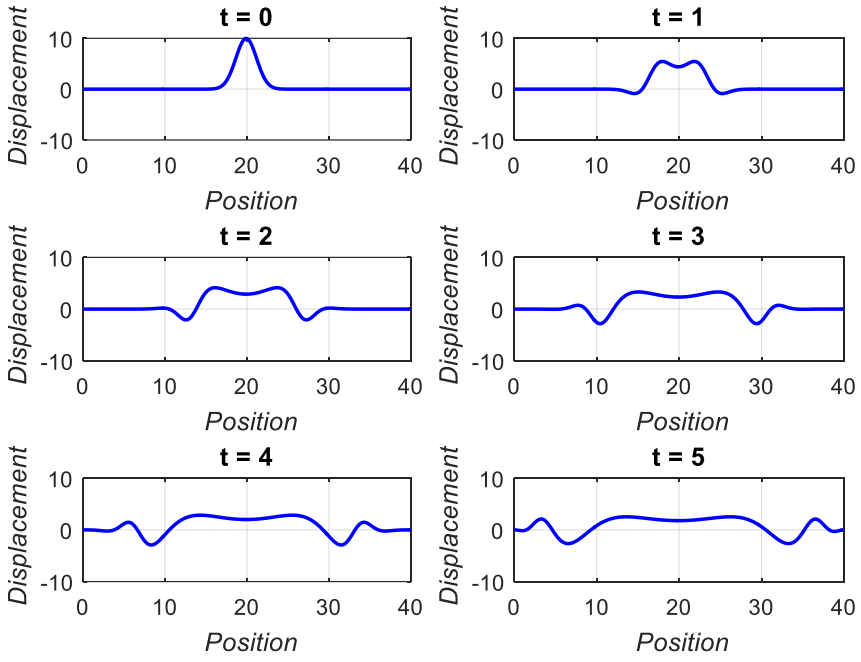

Figure 24: Rayleigh Beam - Finite Element Approximation with 4th Order Runge-Kutta Integration

7.3 Timoshenko Beam Results

As stated previously, the Timoshenko beam theory goes another step beyond the Rayleigh beam theory by accounting for shear deformation. For higher frequency vibration, the Timoshenko beam is the best model. The small displacements caused by the shear deformation and rotary motion are greatly amplified when high frequencies are encountered. Depending on the initial displacement function, the free vibration could experience high frequency vibrations, leading to the prior beam theories giving

inadequate results. Here, we will see how the Timoshenko beam theory compares to the Euler-Bernoulli and Timoshenko beam theory through direct observation of the motion of the beam.

7.3.1 Fourier Analysis

Figure 25, shows the transverse displacement for the Timoshenko beam.

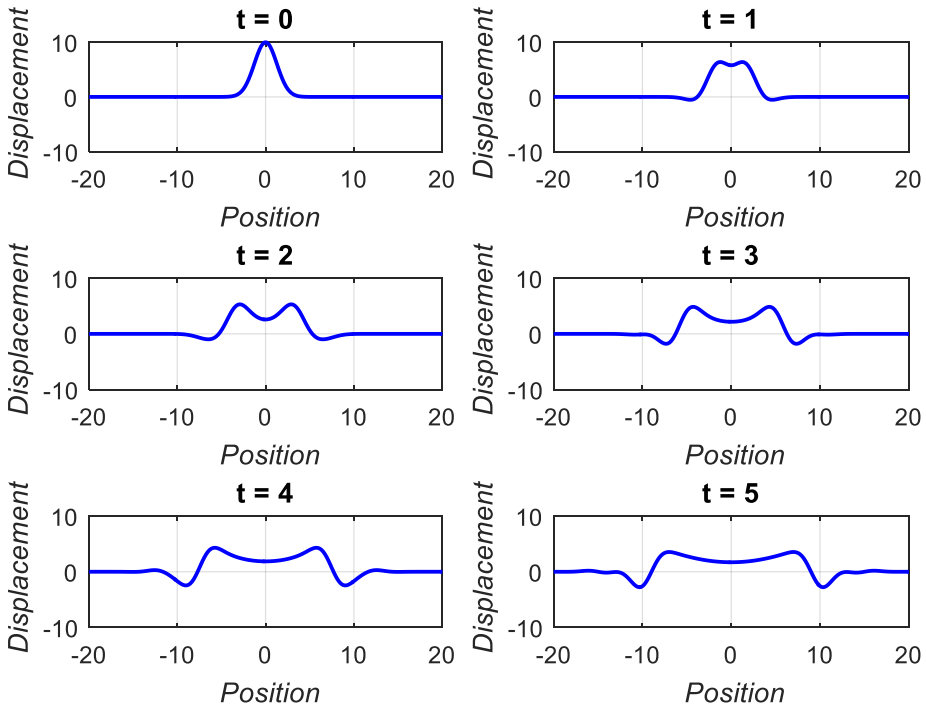

Figure 25: Timoshenko Beam - Inverse Fourier Transform Approximation

Comparing the Rayleigh beam to the Timoshenko beam, there is not much as big of a difference between the two as there is between the Rayleigh beam theory and the Euler-Bernoulli beam theory. We do see some differences of which will be amplified in the coming sections.

7.3.2 Separation of Variables

Using the method of separation of variables, the results in Figure 26 match those in Figure 25 very nicely.

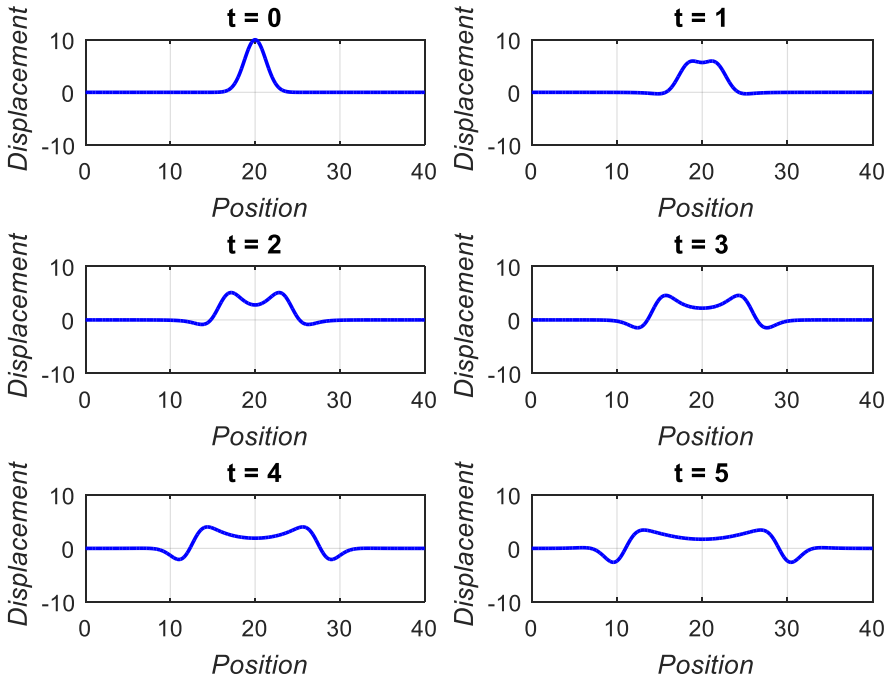

Figure 26: Timoshenko Beam - Separation of Variables - 200 Terms in Series Expansion

7.4 Comparing the Beam Theories

Figure 27 shows the displacement of the beam for all three beam theories together. These results are very interesting as we can see the Euler-Bernoulli beam model traveling much faster. We saw this in the previous sections, but we can see it much better next to the other beam models. The difference between the Timoshenko beam and the Rayleigh beam are also much clearer. It appears the Timoshenko beam has more resistance, due to the shear deformation. It takes longer for the waves to propagate in the Timoshenko beam.

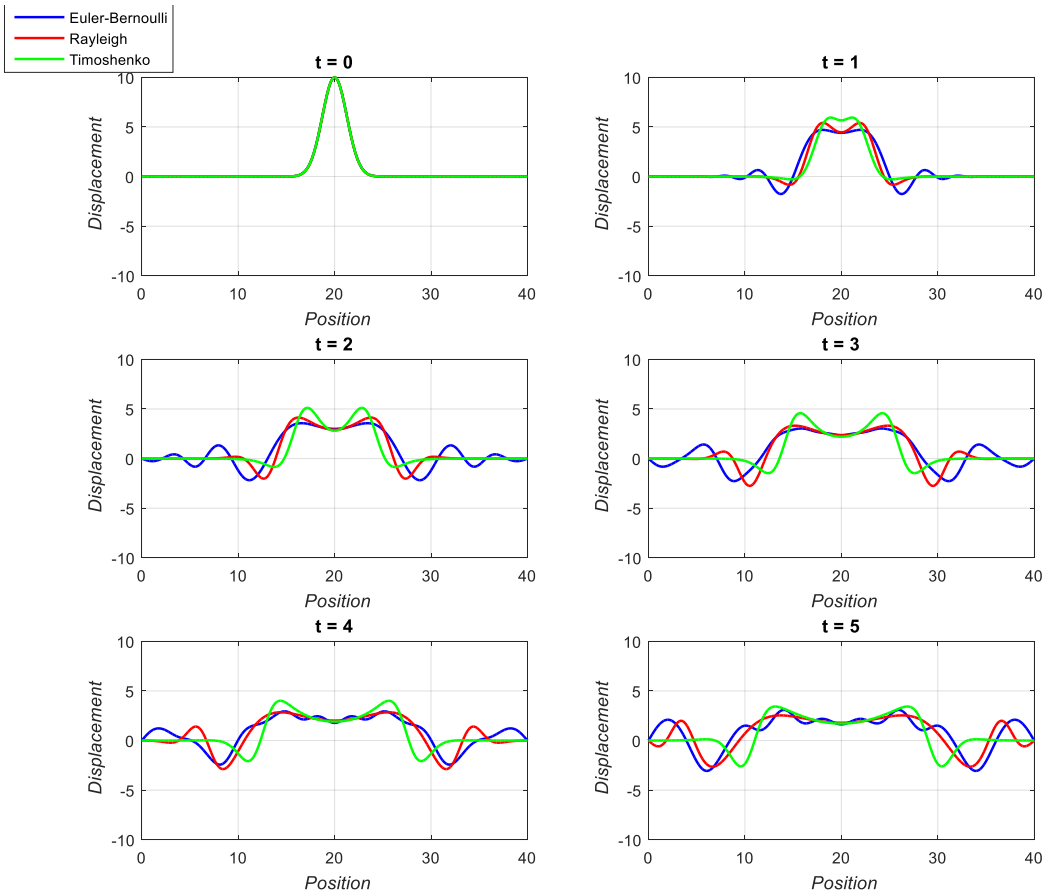

Figure 27: A Comparison Between Beam Theories

8 CONCLUSION

An engineer always strives to be able to verify the solution to the problems they solve. In order to verify the unique problem of wave propagation in beams, multiple numerical techniques needed to converge on the same solution. The Euler-Bernoulli beam has been analyzed with a total of five different methods, all of which prove to converge to the same solution. The convergence is seen visually through the plots in the results, and this is important because the problem has been analyzed in many different way. Through the use of Fourier transforms, we were able to determine an analytical solution, which was then used to verify numerical approximations. The infinite summation that came from the separation of variables method proved to converge to the same results as the Fourier transform solution. As well, using the finite element method with both Newmark's method and the fourth order Runge-Kutta method, we saw the solution converge to the same shape at different time steps.

Although an analytical solution was not obtained for the Rayleigh beam or the Timoshenko beam, the same numerical approximations were used to model the beams. We have seen the numerical approximation techniques converge to the same solution as the analytical solution of the Euler-Bernoulli beam, so confidence has been built that these techniques can be used for the more advanced beam theories. All the numerical methods converged to the same solution for the Rayleigh beam and the Timoshenko beam. Without an analytical solution to the Rayleigh beam or the Timoshenko beam, we cannot truly say that the solutions we have approximated are correct. All we can say is that the results have converged, regardless of the method used to find the solution.

REFERENCES

Haberman, Richard. *Applied Partial Differential Equations with Fourier Series and Boundary Value Problems, Fifth Edition*. New Jersey: Pearson, 2013.

Harrevelt, Seb. "Eigenvalue analysis of the Timoshenko Beam theory with a damped boundary condition." 2012.

Hjelmstad, Keith D. *Fundamentals of Structural Mechanics, Second Edition*. New York: Springer Science+Business Media, Inc., 2005.

Morse, Philip M. *Vibration and Sound, Second Edition*. New York: McGraw-Hill Book Company, 1948.

Sadd, M. H. *Wave Motion and Vibration in Cointinuous Media*. Kingston: University of Rhode Island, Department of Mechanical Engineering & Applied Mechanics, 2009.

Venkatachalam, R. *Mechanical Vibrations*. Delhi: PHI Learning Private Limited, 2014.